Characterization of Swelling and Electroosmotic Transport in Polyelectrolyte Hydrogel Membranes

by

Catherine K. Su

Submitted to the Department of Electrical Engineering and Computer Science

in Partial Fulfillment of the Requirements for the Degree of

Bachelor of Science in Electrical Engineering

at the Massachusetts Institute of Technology

June 1990

Author_____

Department of Electrical Engineering and Computer Science
May 15, 1990

Certified by_____

Alan J. Grodzinsky
Thesis Supervisor

Accepted by_____

Leonard A. Gould
Chairman, Departmental Committee on Undergraduate Theses

Characterization of Swelling and Electroosmotic Transport in Polyelectrolyte Hydrogel Membranes

by

Catherine K. Su

Submitted to the
Department of Electrical Engineering and Computer Science

May 15, 1990

In Partial Fulfillment of the Requirements for the Degree of
Bachelor of Science in Electrical Engineering

Abstract

Dynamic control of solvent flux was studied in a range of synthetic and natural membranes potentially useful for cell immobilization. Augmentation of solvent flux is an important means by which transport of nutrients to cells within the gel membrane can be enhanced. Solvent flux was induced by applying a transmembrane electric field or by applying a pressure gradient. By gravimetric measure of solvent flow, electroosmotic coupling and hydraulic permeability were calculated. The upper and lower values of solvent flux augmentation were measured for two membrane systems, one based on carrageenan and the other on calcium alginate. With these membrane materials, variation of membrane composition can give a continuous range of electroosmotic flow; finer control is possible by changing chemical bath content. Based experiments and a literature review, carrageenan appears to have potential for reliable membrane synthesis and significant capability for electroosmotic augmentation of solvent flux.

Thesis Supervisor: Alan J. Grodzinsky
Title: Professor, Department of Electrical Engineering and Bioengineering

Acknowledgements

Special thanks goes to Professor Al Grodzinsky for his advice and supervision of this project. His dedication to his work and his commitment to students is admired; he always made the time to provide assistance to me whenever I needed it. I want to thank Paul Grimshaw for introducing me to the ancient techniques of gel casting and flux measurement. Thanks also goes to David Chang for the use of his lab and expertise in synthesizing membranes. Finally, I would like to thank everyone else in the lab group for making Continuum Electromechanics such a wonderful place to work.

Contents

List of Figures

List of Tables

Chapter 1

Introduction

1.1 Background

The fixed charge groups of polyelectrolyte hydrogel membranes can be chemically and electrically controlled to effect changes in pore size and thus convection through the membrane. A thorough characterization of a hydrogel membrane's swelling and charge enable finer control of transport through the membrane for a specific application. Electrostatic swelling forces associated with fixed charged groups in the membrane can cause changes in the gel's bulk dimensions and microstructure, causing concomitant changes in transport properties. Further, the presence of membrane fixed charge creates electrophoretic movement of the associated counter-ions that drag solvent through the membrane in a phenomenon called electroosmosis.

Potential applications for a charged membrane include a separation technique for protein purification, controlled release of a drug on demand, and electrical augmentation of nutrient transport in immobilized cell culture. This work studies different synthetic and natural hydrogels for use in establishing a cell matrix that permits electrical control of nutrients. Membranes under investigation include lightly crosslinked membranes made from N,N-(dimethylamino)ethyl methacrylate (DMAEMA) and methyl methacrylate (MMA), agar,

agarose, carrageenan, and calcium alginate. Through observation of the parameters important for electromechanochemical control of swelling and transport, principles may be established that can be useful for tailoring such a membrane system for a specific application.

The development of an electrically controlled solute separation system would benefit diffusion–limited matrices that could also take advantage of selective electrostatic partitioning to purify proteins from cell products and other impurities. Electrical control can achieve significant augmentation of transport and can potentially permit high selectivity in pore size over a continuous range. Charged solutes give an additional basis for separation.

In use as an immobilized cell matrix, the membrane can serve both as a substrate that enhances cell growth and as a screen for cell products. In addition, the development of the microencapsulation process provides a high degree of flexibility between different cell types, purification, and product extraction. Thus, the observed slow initial growth phase in encapsulated cells and diffusion limitations can be compensated through better nutrient access and waste removal in selective electrically-modulated transport system.

1.2 Previous Work

1.2.1 Effects of pH and Ionic Strength on Membrane Permeability

Large changes in swelling and pore size across charged polymer membranes have been induced by altering the chemistry of the surrounding bath. The degree of ionization of the membrane fixed charge groups is modified by pH and other ionic species in the surrounding bath (Ohmine and Tanaka, 1982; Ilavsky, 1981; Cussler, 1988). With decreasing or increasing pH the fixed charge groups, e.g. amino or carboxyl groups, become ionized and create double layer electrostatic forces between the similar charges. These repulsive forces cause the membrane to swell. Similarly, with decreasing external bath concentration the Debye length increases, thereby decreasing the ionic shielding effect; this also causes membrane swelling. For synthetic

gels, the membrane's swelling is limited by the mechanical restoring force produced by the crosslinks. For natural gels the electrostatic bonds limit the swelling.

Ilavsky (1981) analyzed the effect of electrostatic interactions on the polymeric swelling of a polyacrylamide $(PAA)_n$ polyelectrolyte gel, observing that although the fixed charge of the polymer determines the swelling transition, electrolyte and chain flexibility also play a role. A study of the characteristic swelling time of polyelectrolyte gels suggests a correlation to the mechanical diffusion coefficient of the gel network when chemical kinetics are relatively fast (Tanaka and Fillmore, 1979). Freijtas and Cussler (1987) show that temperature also strongly affects swelling.

Weiss *et al.* (1986), Shatayeva *et al.* (1979), and Grimshaw *et al.* (1989) found that changes in bath pH and ionic strength resulted in large, reversible changes in membrane hydration and size-specific permeability in polymethacrylic acid (PMAA) membranes. Similar reversible changes were evident in hydrolyzed polyacrylamide (PA) gels (Gehrke *et al.*, 1986), PA/PMAA copolymer gels (Gehrke and Cussler, 1989), and DMAEMA/MMA copolymers (Siegel, 1988). Membrane composition and cross-link density were found to create limitations in the extent of gel swelling that affected solute permeability (Gehrke *et al.*, 1986; Reinhart and Peppas, 1984; Weiss *et al.*, 1986; Adler, 1988)

1.2.2 Effects of an Applied Electric Field on Solute and Solvent Flux

An applied electric field can alter membrane permeability by regulating ionic concentration profiles to change swelling characteristics or by producing a force on the mobile co-ions within a charged membrane matrix. Changes in intramembrane salt concentration were found to produce a force that modifies the internal double layer repulsion forces between charged groups (Grodzinsky and Shoenfield, 1976; Nussbaum, 1986).

Grimshaw (1989) presented a macroscopic continuum flow model that describes the dominant electrochemical forces affecting flux and swelling forces in PMAA membranes. These mechanisms, present under different charged membrane conditions, are (1) electrodiffusion,

which alters membrane charging and swelling, (2) electroosmotic convection, and (3) electrophoresis of a charged solute.

1.2.3 Use of Various Polyelectrolyte Gels

DMAEMA/MMA membrane. Previous experiments indicate the feasibility of using semipermeable polymeric membranes to encapsulate cells for *in vivo* and *in vitro* application. Sefton *et al.* (1987) reported the first successful encapsulation of live mammalian cells into this polymer. The cell viability in differing concentrations of DMAEMA, MMA, HEMAS, and MA polymers were studied (Gharapetial *et al.*, 1986; Sefton *et al.*, 1987). Sefton *et al.* (1987) further suggested that cell growth and viability was limited to areas of adequate nutrient diffusion and that the tertiary amine of the dimethylethyl group permitted increased growth of anchorage-dependent cells.

Siegel and Firestone (1988) conducted experiments illustrating the swelling dependence of MMA/DMAEMA membranes on pH, concluding that as the proportion of MMA to DMAEMA increases the pH of swelling transition shifts to a lower pH and the extent of swelling decreases. Their experiments indicated a sharp transition in swelling at a particular pH. Firestone and Siegel (1988) showed pH-dependent swelling kinetics where a slower swelling dynamics occurred from a less hydrated state.

Polyacrylate encapsulation. In the development of polyacrylate cell matrices, immobilized entrapment of enzyme-forming cells has been studied extensively. The viability and rate of enzyme production was studied for bacteria immobilized in polyacrylamide gels (Mosbach and Larsson, 1970; Slowinski and Charm, 1973). Freeman and Aharonowitz (1981) demonstrated higher cell viability and enzyme production by cells suspended in preformed polyacrylamide chains that allowed crosslinking to occur in cold, neutral conditions. Siess and Divies (1981) observed that polymerization destroyed 40% to 80% of immobilized yeast cells with 75% to 85% of them losing their integrity; after a long adaptation period cells immobilized in the matrix lost viability as a result of insufficient nutrients while those at the

periphery thrived, yielding a high fermentation rate. Morikawa *et al.* (1980) showed that bacteria production of bioactive products is higher in immobilized whole-cell systems than those kept in conventional continuous fermentation process. Immobilized cells systems suffer a shorter half-life, where gel surface cell growth decreased productivity by preventing the diffusion of oxygen and nutrients.

κ-carrageenan. Carrageenan is a hydrocolloid consisting mainly of calcium sulfate esters of galactose and 3,6-anhydro-galactose copolymers. The relative proportion of cations varies depending on the processing (FMC Sourcebook). It contains high characteristic charge and has been shown to be compatible for cell immobilization of bacterial and microbial cells. Yamamoto (1980) described encapsulated cells as having enhanced enzymatic activity and increased operational stability, concluding that the simplicity of the immobilization process and the high mechanical strength of the preparation make carrageenan ideal for industrial enzymatic production. Baudet (1983) similarly noted the high steady-state cell density, finding that growth occurs on the surface of the beads due to nutrient diffusion limitations.

Calcium alginate. Alginate, a heteropolysaccharide derived from brown seaweed, is used to immobilize a variety of mammalian and microbial cells. Alginate forms gels by reaction with calcium salts where ribbon-like segments of alginic acid stack upon one another, linked by calcium ions. Thus, under mild conditions gels may form; they may be dissolved by competing away the calcium ion. In addition, the gels can be formed in a wide variety of configurations such as spheres, films, or fibers.

Immobilized cells permit continuous addition of substrate and extraction of product in a system that requires less medium and achieves higher final cell densities. Domurado *et al.* (1988) immobilized nontransformed lymphocytes into alginate beads to observe diffusion-limited viability of the cells. The explanation lies in the differential diffusion coefficients of protein molecules from the alginate beads to the medium and from the medium into the alginate (Tanaka *et al.*, 1984). In another study, Tompkins *et al.* (1988) observed similar detoxification reaction rates between alginate-immobilized and nonimmobilized hepatocytes, concluding that transport limitations do not occur. Further, the urethene-coated alginate-

immobilized hybridoma cells created by Iijima *et al.* (1988) achieved even higher cell densities and greater monoclonal antibody yield.

An alternative cell immobilization technique, microencapsulation, entraps viable cells within semipermeable microcapsules that permit the diffusion of small molecules such as oxygen, glucose, and nutrients but block the passage of large molecules and cells. Alginate poly-l-lysine has been used to microencapsulate cells. Lim and Sun (1980) microencapsulated islets into rats to correct a diabetic state. Gilligan *et al.* (1987) have produced monoclonal antibodies from encapsulated hybridoma cells where cells grew to a density comparable to extracapsular cells but achieved higher purity. Furthermore, membrane permeability can be adjusted to retain the high molecular weight bioactive protein product and allow diffusion of the low molecular weight enzymes into the extracapsular medium (Duff, 1985). Thus, microencapsulation permits purification before harvest.

1.3 Overview of Present Work

This work focuses on characterization of the electrical parameters in various hydrogel systems to better evaluate constraints in the dynamic control of solvent and solute transport. In doing so, suggestions can be made towards a hydrogel to be used for a cell immobilized matrix. By measuring fluid transport across the membrane in response to a transmembrane electric field or a pressure gradient, the electroosmotic coupling coefficient and the hydraulic permeability can be calculated. These variables give the electrically-enhanced solvent flux and an estimate of the pore size, respectively. By further assuming a macroscopic model where the Debye length is greater than the pore size and given the membrane hydration, the charge density may also be calculated. These parameters give valuable information for selecting a membrane for a specific application.

Chapter 2

Theoretical Model of Transport Mechanisms

2.1 Solvent Flux

2.1.1 Electromechanical force

In fluid dynamics Darcy's law, $U = -k' \frac{\partial P}{\partial x}$, states that whenever there is fluid flow a pressure gradient must exist where pressure and flow are related by a hydraulic permeability k'. The relation between mechanical forces and flows associated with changes in membrane hydration can be described by an expanded Darcy's law,

$$U = -k'[\frac{\partial P}{\partial x} + z_m \bar{c}_m F E] \tag{2.1}$$

where the electroosmotic force $z_m \bar{c}_m F E$ contributes to the flow by a constant identical to the pressure gradient in the macrocontinuum model. Using the Navier-Stokes equation with

the assumption that the fluid drag forces replace the viscous forces, $-\frac{U}{k'} - \nabla P_f + \rho_u \mathbf{E} = 0$, the permeability coefficient for both forces are identical (Frank *et al*, submitted). Equation 2.1 describes interstitial fluid flow (**U**) relative to a solid membrane matrix driven by a gradient in fluid pressure ($\frac{\partial P}{\partial x} = \frac{\rho g \triangle h}{\delta}$) or an electric field **E** to produce the electroosmotic force $z_m \bar{c}_m FE$. Because of the electrically-induced membrane deformation, the hydraulic permeability k' may depend on hydration. Another constant, the electroosmotic coupling coefficient k_i is used to describe the relation between fluid flow and the applied current density.

By assuming continuity of fluid volume in the steady state,

$$\frac{\partial H}{\partial t} = -\frac{\partial(\alpha U)}{\partial \psi} = 0 \tag{2.2}$$

U is a constant flow everywhere in the membrane. Thus, electroosmosis across a uniform membrane creates no internal pressure gradients since the charge density and field exactly cancel the flow. In the absence of both internal and external pressure gradients the electroosmotic solvent flow rate is described by

$$U = -k' z_m \bar{c}_m FE = k_i J \tag{2.3}$$

where **J** is the applied current density. The electroosmotic coupling coefficient k_i can be found by direct measurement of the electroosmotic solvent flux across the membrane.

2.1.2 Electroosmotic Coefficients

The electroosmotic coupling coefficient is defined as

$$k_i = \frac{-k' z_m \bar{c}_m}{\phi \Sigma \bar{\mu}_i |z_i| \bar{c}_i + k' (z_m \bar{c}_m)^2 F} \tag{2.4}$$

which relates the field **E** to the applied current density **J**. They are related by the intramembrane ionic content $\Sigma \bar{\mu}_i |z_i| \bar{c}_i$ and the square of the membrane charge density $\rho_m = z_m \bar{c}_m$. Thus, for highly charged membranes the electrostatic coupling is inversely related to the mem-

brane charge and for low charge membranes, the electrostatic coupling is directly related to charge.

2.1.3 Electric Field Effect on Membrane Charge

A one-dimensional continuum model has been used to describe the underlying mechanism of electromechanical deformation of a membrane. These electromechanical changes correspond to changes in the hydration of a polyelectrolyte due to transmembrane electric fields which alter the ionic environment. This model describes changes in ionic strength that correspond directly to transport, swelling, and electrodiffusion in the membrane.

The model is primarily based upon two equations that describe the electrochemical dynamics of charged groups. The first, the time-varying flux equation is

$$\Gamma_i = \phi(-\bar{D}_i \frac{\partial \bar{c}_i}{\partial x} + \bar{\mu}_i \bar{c}_i \mathbf{E}) + \bar{c}_i \mathbf{U} \tag{2.5}$$

where $\bar{c}_i$ is the intramembrane concentration of ion i having an intramembrane diffusivity of $\bar{D}_i$ and electrical mobility $\bar{\mu}_i$, ϕ is the membrane porosity, $\mathbf{E}$ the local electric field, and $\mathbf{U}$ is the total area-averaged fluid velocity. The equation has three terms that describe, in order, the effects of diffusion, migration, and convection. The second equation is the continuity condition. It is

$$\frac{\partial}{\partial t}(H\bar{c}_i + H\bar{c}_i^b) = -\frac{\partial \alpha \bar{\Gamma}_i}{\partial \psi} \tag{2.6}$$

where ψ is the Lagrangian coordinate frame associated with the solid membrane matrix, α is the total membrane area normalized by the zero-hydration area, H is the local membrane hydration, $\bar{c}_i^b$ is the concentration of ion i reversibly bound to the membrane charge groups.

By assuming electroneutrality and the presence of two oppositely-charged ions of which one dominates in the bulk, we have two equations that will enable us to solve for the two boundary conditions. The electroneutrality condition $\bar{\rho}_m + \Sigma z_i \bar{c}_i = 0$ for the two-ion system described above yields $\bar{c}_+ + \bar{c}_- + \frac{\bar{\rho}_m}{F} = 0$ where $\frac{\bar{\rho}_m}{F}$ is the total charge density of the

membrane. The Boltzmann boundary condition relating the free ion concentration in the membrane ($\bar{c}$) and bath (c) to potential differences between the intramembrane space and bath $\bar{c}_{\pm} = c'_{o\pm} \exp(-zF\phi/RT)$ written in terms of the activity coefficient $\gamma_{\pm}$ yields the relation $\frac{(\bar{\gamma}_{\pm})^2}{(\gamma_{\pm})^2}(\bar{c}_+)(\bar{c}_-) = c_o^2$ where the activity coefficients can be assumed to be unity.

Based on the continuity and flux equations, the entire differential equation for the time-varying space-dependent concentrations can be written. The bulk electroosmotic flow presented as the convection term in the flux relation may be modeled by the continuum, phenomenological relation

$$U_x = -k' z_m \bar{c}_m F \mathbf{E}_o = k_{12} \nabla V = -k_{12} \delta \mathbf{E}_o \tag{2.7}$$

defined for $E_o > 0$ and $\bar{\rho}_m > 0$ where k_{12} is the electroosmotic transduction coefficient. Combining equations (2.5) and (2.7) for $\frac{\partial}{\partial \psi} = \frac{\partial}{\partial x}$, we obtain

$$\begin{aligned} H\frac{\partial \bar{c}_i}{\partial t} &= -\frac{\partial}{\partial \psi}\alpha[-\phi \bar{D}_i \frac{\partial \bar{c}_i}{\partial x} + \bar{c}_i E_o(\bar{\mu}_i \phi - k_{12}\delta)] \\ &= \alpha\phi \bar{D}_i \frac{\partial^2 \bar{c}_i}{\partial x^2} - \alpha\phi \bar{\mu}_i E_o[1 - \frac{k_{12}\delta}{\bar{\mu}_i \phi}]\frac{\partial \bar{c}_i}{\partial x} \end{aligned} \tag{2.8}$$

In these equations, we have assumed that the diffusivity, mobility, and activity coefficients of the co-ion remain constant across the membrane.

2.2 Overall Solute Transport

In the absence of spatial gradients in chemical and mechanical parameters the flux equation (2.5) can be rewritten to model the contribution of electroosmosis and electrophoresis on solute transport. Under these conditions, the flux used for solute transport can be written as

$$\Gamma_s = \phi \bar{D}_s (\frac{\partial \bar{c}_s}{\partial x} + \frac{P_e}{\delta_o}\bar{c}_s) \tag{2.9}$$

where δ_o is the initial membrane thickness and P_e is the effective Peclet number. The Peclet number for a solute, combining the effects of electrophoresis and electroosmosis, is defined as

$$P_e = \delta_o\left(\frac{\phi\bar{\mu}_s E + W_s U}{\Phi \bar{D}_s}\right) \tag{2.10}$$

where W_s is the convective restriction factor and the electrical mobility $\bar{\mu}_s$ can be determined from the Nernst-Einstein relation

$$\frac{D_s}{\mu_s} = \frac{RT}{z_s F}. \tag{2.11}$$

Combining the flux equation with the continuity equation completes the one-dimensional continuum model that explains the magnitude and kinetics of electrically-induced changes in flux across the membrane. This yields

$$\frac{\partial \bar{c}_s}{\partial t} = \bar{D}_s\left(\frac{\partial^2 \bar{c}_s}{\partial x^2} + \frac{P_e}{\delta_o}\frac{\partial \bar{c}_s}{\partial x}\right) \tag{2.12}$$

where the flux can be related to the membrane thickness, the Peclet number, and the diffusivity.

Chapter 3

Materials and Methods

3.1 Membrane fabrication

Membrane composition was chosen on the basis of biocompatibility and membrane fixed charge groups. Originally, DMAEMA was chosen as the primary model system because of its successful use for growth of mammalian cells by Sefton *et al.* (1987) and the flexibility in altering its charge density. While a range of charged copolymers were being studied, constraints in cell encapsulation procedures shifted the investigation towards natural polymers. Although consistency of charge and repeatable measurement was a problem in the characterization of agar membranes, other potentially suitable materials have been studied and described.

DMAEMA/MMA Membrane. (Dimethylamino)ethyl methacrylate (DMAEMA) and methyl methacrylate (MMA) gels were synthesized by bulk copolymerization to produce gels containing one-tenth percent crosslinker per monomer. Copolymers were formed by combining a specified composition of DMAEMA monomer (Aldrich, Inc.) with MMA monomer (Polysciences, Inc.). This solution along with 0.1% w/w AIBN initiator and 0.5% w/w divinyl benzene crosslinker (Polysciences, Inc.), was pipetted between two glass plates with a PTFE

(Teflon) spacer of known thickness. The bottom plate was first covered with teflon-coated foil to facilitate removal of the membranes.

The unpolymerized membrane sandwich was clamped together, insuring that all air bubbles were removed, rinsed in water, and placed in a 60°C water bath for eight hours. When polymerization was complete the membrane attached to the top plate was soaked in deionized water overnight. After that time the membrane was rolled off the glass plate to be soaked for an additional day in deionized water to remove impurities. Membranes were kept refrigerated in 100 mM KCl. Prior to any experimentation the membranes were equilibrated overnight in the experimental bath solution.

With this synthesis procedure, synthetic DMAEMA gels were produced with various concentrations of fixed charge groups. This parameter was controlled by varying the molar ratios of DMAEMA to MMA. The designation for membrane composition is Sx n/m DMAEMA/MMA where n and m are the mole ratios of DMAEMA and MMA respectively and x is one-tenth percent crosslinker. DMAEMA/MMA copolymers of 100/0, 90/10, 75/25, 60/40, and 45/55 mole % were formed.

Natural Hydrogel Membranes. Agar was obtained from Difcoe (Detroit, Michigan), SeaKem LE agarose from FMC Chemicals (lot 60320 in Rockland, Maine), and κ-carrageenan from Sigma Chemical Company (lot 19F0637 in Missouri). These hydrogels were made by mixing the desired amounts of each powder in deionized water and heating the mixture in an autoclave for 10 minutes at 110°C and 21 psi. The homogeneous solution was kept stirring in a hot water bath while a few milliliters were pipetted between two glass plates separated by a 500 μm PTFE o-ring spacer. Since the solution was quite viscous, gelling quickly, air bubbles were removed from the bottom plate before overlaying the top plate.

Since Ca-alginate gels form when alginic acid contacts divalent cations, two solutions were made. First, sodium alginate (Sigma Chemical Co, lot 11F0168) was dissolved in deionized water (w/v ration). A solution of 1% $CaCl_2 \cdot 2H_2O$ was also mixed. Then a filter paper soaked in calcium chloride was placed in a petri dish, followed by 9 milliliters or 1 mm height of alginate solution. Another $CaCl_2$–soaked filter paper was settled on top of the alginate

topped with 6 mls 1% $CaCl_2 \cdot 2H_2O$ solution, another filter paper, and a teflon disk. As the Ca^{2+} ions diffused into the matrix of sulfate ions, the gel formed. Some pressure was applied to the top to maintain smooth surfaces. After half an hour the filters were removed and the gel stored in 1% $CaCl_2 \cdot 2H_2O$ for at least 24 hours. The fabrication method was adopted from that described by Krouwel *et al.* (1982).

The chemical structure of all polymers are shown in Figure 3-1. As illustrated MAA and alginate contain one carboxyl group per monomer. The dominant charge on DMAEMA is a single amino group and the dominant charge on carrageenan is a single sulfate group. Agarose and MMA are generally considered neutrally charged.

3.2 Membrane Thickness Measurement

Although membranes were cast to a known thickness, natural hydrogels tend to shrink as they solidify and all membranes tend to swell in salt solution. To determine the thickness of membrane for a particular hydration condition after it was cast, the equilibrated membrane's thickness was measured using an ohm meter and a micrometer. The calipers were closed on the membrane until a low resistance was measured. Taking the preliminary reading from the micrometer, the calipers are opened again just until an open circuit resistance is observed and then closed slowly until the calipers just touch the membrane. That measure represents the thickness of the membrane.

3.3 Membrane Hydration Measurement

An important mechanism that affects transport properties is the control of membrane permeability through bulk changes in hydration (Grimshaw, 1989). Due to the presence of ionizable fixed charge groups, altering the pH can cause swelling or shrinking of the membrane. Altering the external bath concentration alters the Debye length affecting ionic shielding and thus

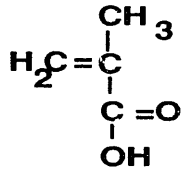

MAA

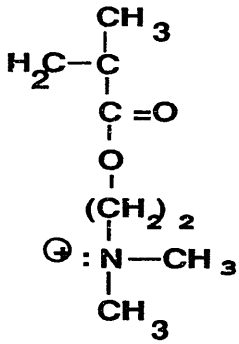

DMAEMA

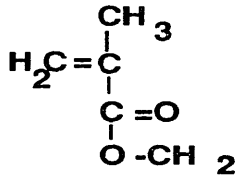

MMA

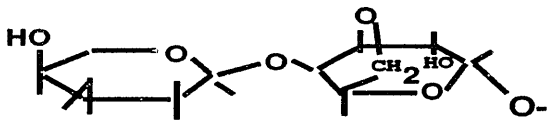

AGAROSE

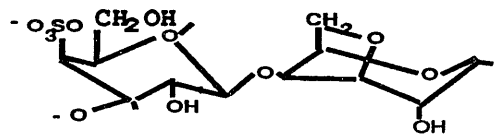

K-CARRAGEENAN

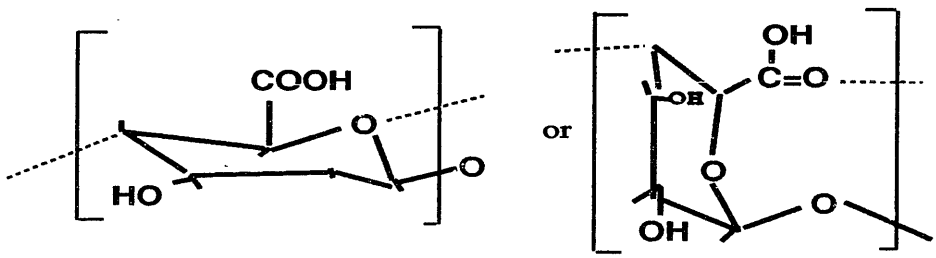

ALGINIC ACID

Figure 3-1: Single unit structure of polymers. Synthetic polymers MAA, DMAEMA, and MMA are crosslinked with either triethylene glycol dimethacrylate (MAA) or divinyl benzene. The natural membranes consist of chains attached by glycosidic bonds with gel crosslinked with electrostatic and hydrogen bonds between charged groups.

swelling. In such a manner the extrinsic factors of pH and ionic concentration can control the intrinsic variables of fixed charge and the associated changes in hydration. To characterize the degree of swelling associated with changes in ionization of DMAEMA/MMA the equilibrium hydration of each polymer was measured as a function of pH. Potentiometric titration of the DMAEMA monomer indicates a pK_b of 7.7 (Skatkay and Michaeli, 1966). Other membrane hydration values were measured at neutral pH.

Equilibrium Hydration of DMAEMA/MMA. Cylindrical disks (1.5 cm in diameter) were punched out from a membrane and equilibrated in a potassium chloride salt solution of constant pH. Five DMAEMA/MMA membranes (volume to volume ratios 100/0, 90/0, 75/25, 60/40, and 45/55) were cast to a thickness of 500 μm at pH 6 such that the neutrally-charged membranes would acquire a net positive charge with a decrease in pH.

Samples of all five membrane types were placed within a specially designed nylon mesh carrier to be immersed in a single bath solution of 100 mM KCl (Figure 3-2). Bath solutions were monitored by a microcomputer's closed loop feedback system to maintain pH via acid and base Dosimat burets and a pH electrode. When the added acid and base (HCl and KOH) increased the bath ionic content by more than 0.5%, a bath equilibrated to the same pH was substituted. Constant stirring kept the solution recirculating to preserve homogeneity of ionic concentrations within the bath.

The membranous disks were placed in the nylon carrier in duplicate. Every 3–4 hours each disk was removed from solution, blotted with a tissue, and weighed in a covered dish. Because of variation in fixed charge, the membrane disks used in testing were conditioned to the proper pH to maintain constant swell size before weight measurements were taken. At 8 different pH values equilibrium weight measurements were obtained. Membranes were then neutralized at high pH , washed in deionized water to remove salts, dried under vacuum, and weighed. Hydration is defined as the ratio of fluid weight to dry polymer weight. The equation is defined as follows where W_d is the dry polymer weight and W_w is the swollen weight.

$$H = \frac{W_w - W_d}{W_d} \tag{3.1}$$

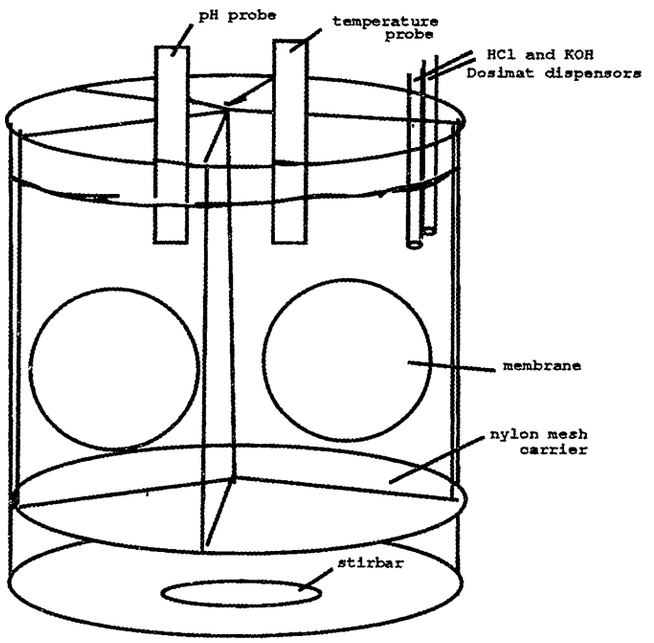

Figure 3-2: Apparatus for maintaining constant pH and low ionic content during swelling equilibration of DMAEMA/MMA copolymers.

Although equilibrium hydration was being assessed, the single container apparatus provided identical bath conditions to all membranes. Thus, the relative rate of swelling of different membranes contained in the bath can be compared.

Equilibrium hydration of natural hydrogels. Since transport experiments were conducted at pH 7 in 100 mM KCl, the hydration of the natural hydrogel membranes were measured exclusively at that pH. This allowed a comparison of the differences in hydration between membranes and an estimate of charge density. Membranes were placed in a beaker at pH 7 in 100 mM KCl and 1 mM phosphate buffer. After several days, a wet weight was measured as previously described. Membranes could not be fully neutralized since natural polymers are sensitive to extremes in pH. The membranes were placed in KCl solutions at pH 8–8.5, washed thoroughly in deionized water, and dried under vacuum to obtain a dry polymer weight.

3.4 Transport Measurement Procedure

A series of transport experiments were designed to investigate selective changes in transmembrane solvent and solute flux induced by changes in bath chemistry and upon application of a transmembrane electric field. The extent of electroosmosis in membranes was evaluated by direct measurement of the solvent flux in response to an electric field. It was possible to simultaneously measure solute flux using spectophotometer reading of fluorescently-dyed molecules placed in the bath.

Apparatus. The transport apparatus was that used by Grodzinsky *et al.* (1976) to measure electromechanical force transduction in collagen. The membrane, pre-equilibrated overnight in the bath solution, was surrounded by rubber o-rings and clamped between two half cells of acrylic plastic (Figure 3-3). A membrane area of 3.14 cm^2 was exposed on both sides to 250 ml bath solutions. Each half cell was filled with electrolyte of the desired pH and the entire apparatus rested on two magnetic stirplates. A transmembrane electric field was produced by a constant DC current source via a pair of salt bridge electrodes placed in the baths; the polyacrylamide salt bridges prevented the platinum electrode reaction products from contaminating the bath. The baths, continually stirred with magnetic stirbars, may also contain pH and temperature probes to regulate and monitor pH and temperature.

Solvent Flux: Electroosmosis Transport To measure the solvent flux the downstream side of the transport apparatus was completely sealed to the atmosphere (Figure 3-4). Tubing connected the downstream bath to a covered beaker of bath solution placed on top of a microgram balance (Sartorius Research, Gottingen, Germany). Transmembrane solvent flux was determined from the rate of change of the measured weight.

To yield consistent weight measurements, evaporation from the beaker was minimized and potential leaks in the transport cell sealed. To suppress evaporation from the beaker, the beaker was partially covered and a humid atmosphere was maintained in the covered weighing

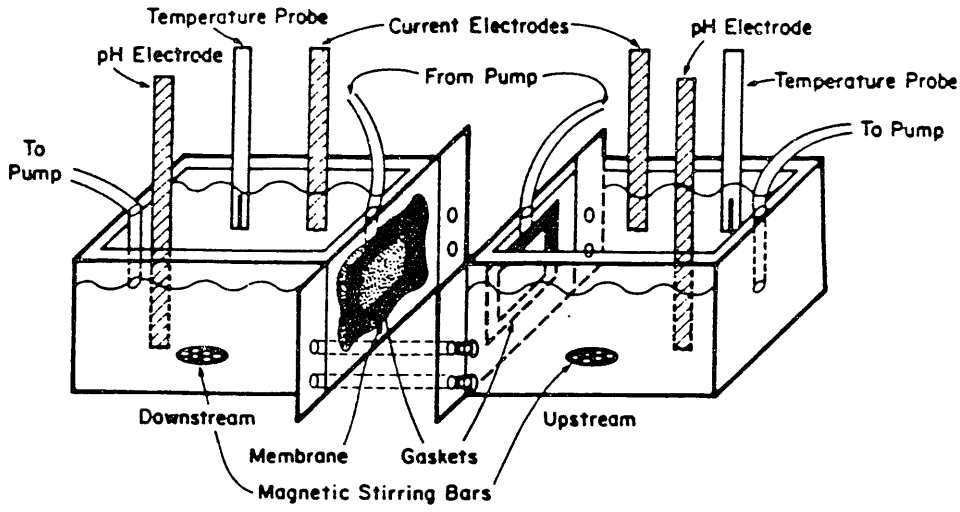

Figure 3-3: Transport apparatus for measuring solvent and solute flux across the membrane in response to chemical or electrical perturbation (Grimshaw, 1989).

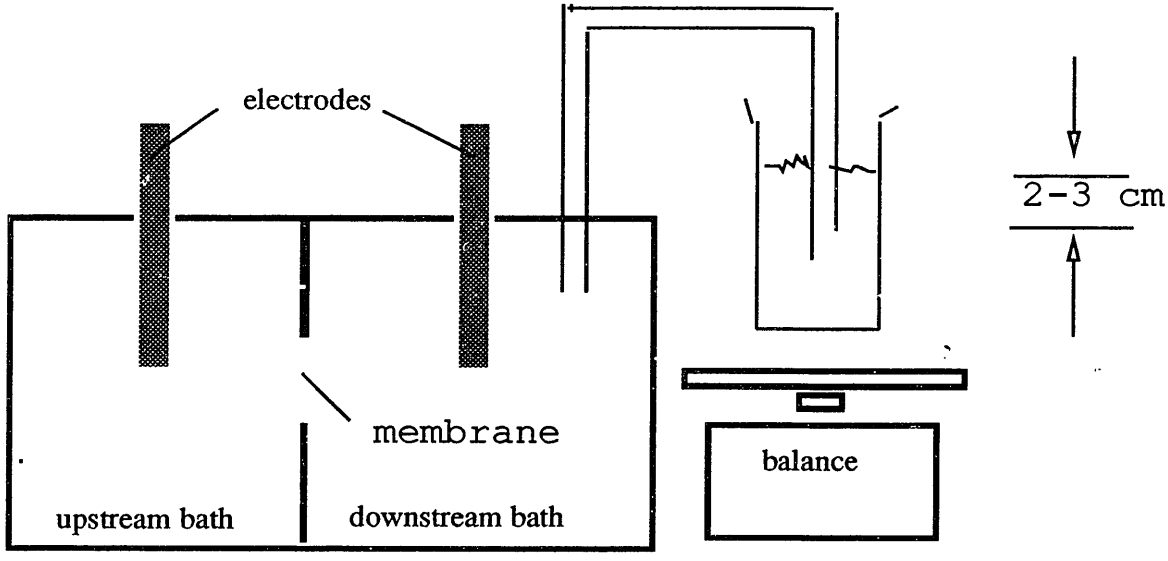

Figure 3-4: Apparatus for measurement of electroosmotic solvent flux across membrane disks. The membrane was held between two baths, labelled upstream and downstream. Each transport half-cell was mounted on a stir plate.

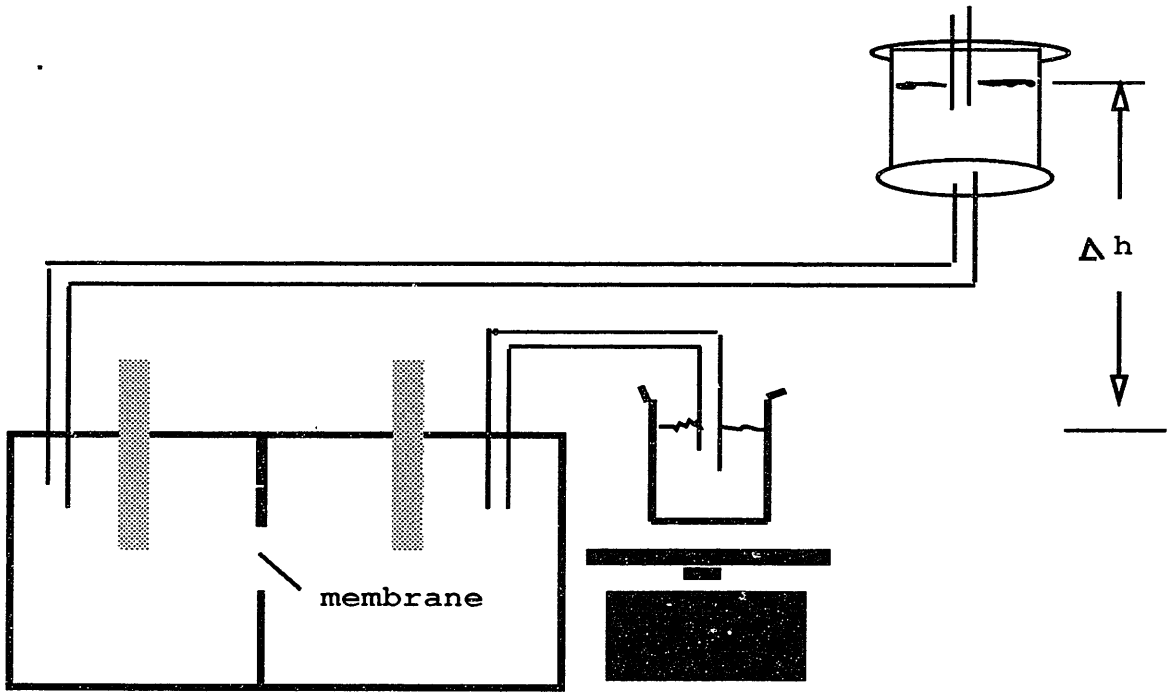

Figure 3-5: Modified transport apparatus to permit measure of hydraulic permeability and electroosmotic solvent flux under a constant, known pressure gradient. The entire transport apparatus was closed to the atmosphere with a constant pressure chamber attached to the upstream side.

area by keeping a second beaker of water in the vicinity. Temperature and pH probes were not used, made unnecessary by the short duration of each experiment and buffering the bath solution.

3.5 Solvent Flux: Constant Pressure Gradient

To measure the hydraulic permeability and to maintain a fixed pressure gradient across the membrane a constant pressure vessel (Pharmacia Fine Chemicals, Holland) was connected to the upstream side of the transport cell (Figure 3-5). With this setup, by vertically moving the pressure vessel a known pressure gradient was established across the membrane.

To begin the experiment $\triangle$h was adjusted to control flow in both directions, insuring that no leaks existed anywhere in the system. Then, a barely perceptible steady state flow was established, to insure that any field-induced flow was not masked by the pressure-induced flux. Current densities of 7 to 10 minutes duration were applied sequentially of strengths -300, -100, 0, 100, and 300 A/m^2. Each field strength was then repeated to check that a consistent result was originally obtained. Then, to measure hydraulic permeability a larger fluid gradient $\triangle h$ of 10-40 cm was established across the membrane.

Chapter 4

Experimental Results: Membrane Characterization

Using the apparatus of Figure 3-2, the swelling of various copolymers of DMAEMA/MMA were measured with changes in pH. The hydrated membranes were kept in the bath of fixed pH until the measured weight remained stable. Then, the bath pH was changed to allow the hydrogel membrane to attain a new equilibrium.

4.1 Equilibrium Hydration

The equilibrium hydration measurements for differently charged hydrogels are graphed in Figure 4-1. A dramatic change in hydration (ratio of fluid to polymer weight) of DMAEMA/MMA membranes is evident between pH range 7.8 to 8. At low pH the amino groups are ionized and the membranes are in a highly swollen state. As pH is increased, the amino groups become neutralized and membrane swelling decreases.

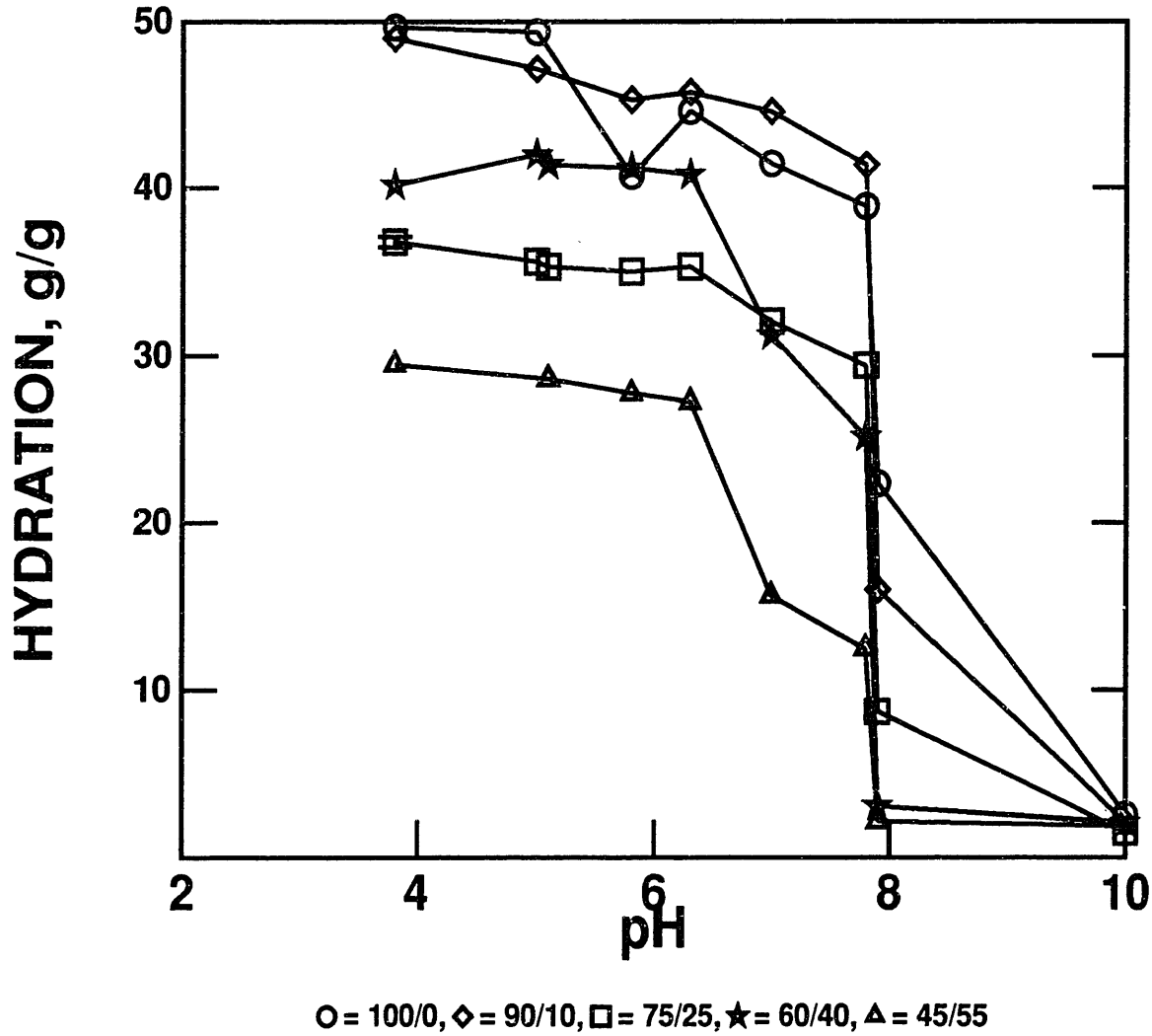

Figure 4-1: Equilibrium membrane hydration of DMAEMA/MMA copolymer membranes kept in 100 mM KCl bath solution with pH regulated using 0.25 M KOH and 0.25 M HCl Dosimats. 100/0, 90/10, 75/25, 60/40, and 45/55 (mole/mole ratio) DMAEMA/MMA hydration versus pH.

pH	DMAEMA/MMA ratio				
	100/0	90/10	75/25	60/40	45/55
5.8	22.6	17.1	6.08	2.85	1.49
3.8	49.7	49.0	36.8	40.2	29.5
5.1	49.4	47.2	35.3	41.4	28.6
5.0	49.4	47.2	35.6	42.0	29.5
5.8	40.7	45.3	35.0	41.2	27.8
6.3	44.6	45.8	35.3	40.8	27.3
7.0	41.4	44.6	32.1	31.2	15.5
7.8	38.9	41.4	29.4	25.2	12.5
7.9	22.4	16.0	8.69	3.06	2.13
10.0	2.54	2.03	1.50	2.06	1.84

Table 4.1: Equilibrium hydration (weight/weight) of DMAEMA/MMA copolymers. These values are sketched in Figure 4-1.

The membranes were initially kept refrigerated at pH 5.8 when the experiment began. Equilibrium hydration values are recorded in Table 4-1, beginning with the refrigerated hydration value where the cold temperature can account for the lower hydration. Otherwise, the bath temperature varied between 27° and 29°C. Pure DMAEMA hydration ranges from 2 to 50 while 45/55 DMAEMA/MMA hydration ranges from 2 to 30. Surprisingly, the 60/40 DMAEMA/MMA swelled more than the 75/25 copolymer. The neutralized membranes all had approximately the same hydration; only the maximum hydration varied by composition. Dry weights for the 1.5 cm disks were 0.0177g, 0.0216g, 0.0339g, 0.0493g, and 0.0584g for 100/0, 90/10, 75/25, 60/40, and 45/55 (m/m) DMAEMA/MMA respectively, indicating that the higher the MMA composition the higher the polymer weight.

4.2 Nonequilibrium Hydration

Shrinking and swelling kinetics were observed in DMAEMA/MMA copolymers for step changes in pH. Using 500μm thick membranes, bath pH was altered to achieve each equilibrium point tabulated in Table 4-1 and graphed in Figure 4-1. The transient swellings data (Figure 4-2) shows that pure DMAEMA swells faster than the copolymers, attaining a constant weight most quickly.

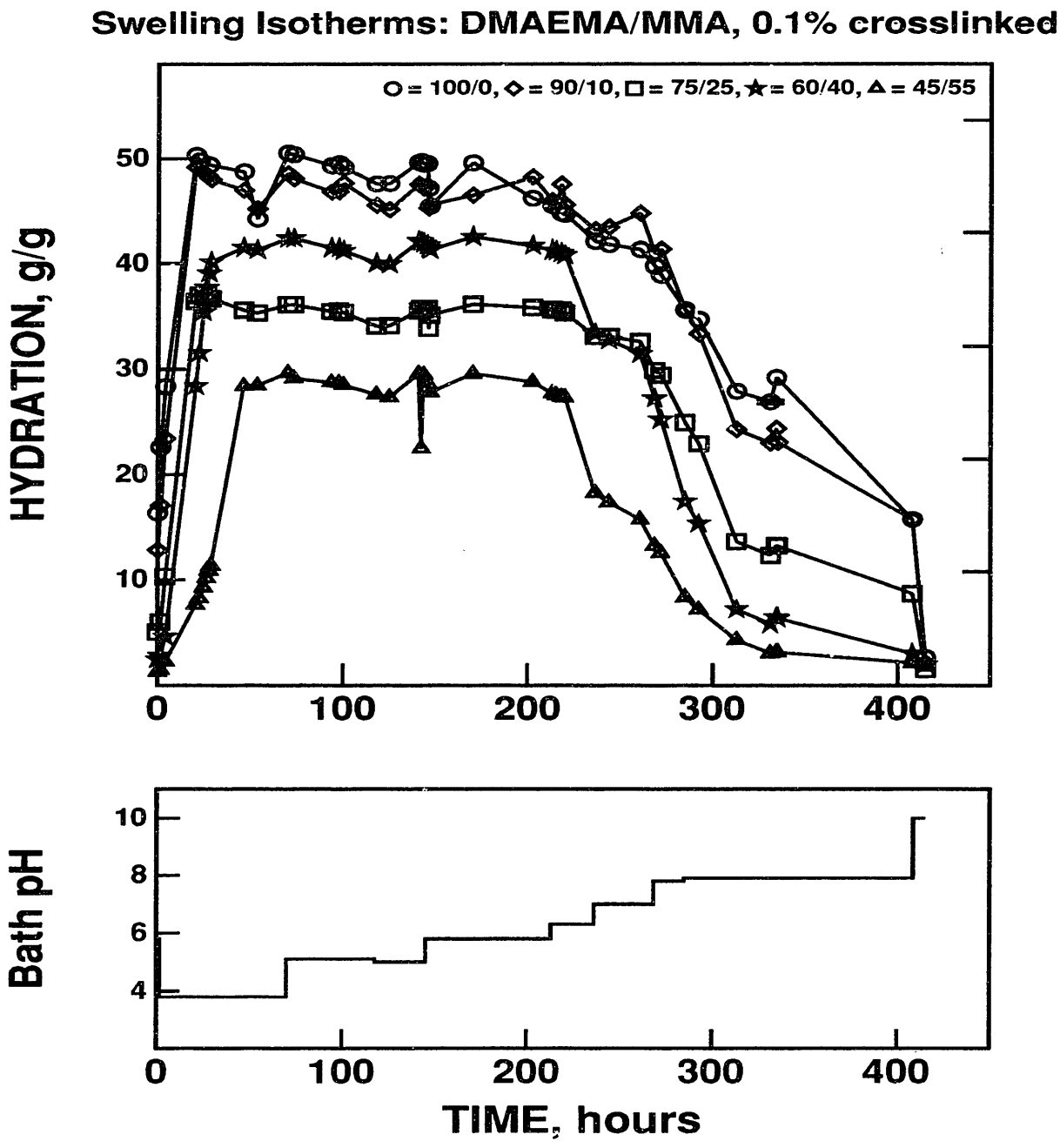

Figure 4-2: Hydration kinetics of 100/0, 90/10, 75/25, 60/40, and 45/55 DMAEMA/MMA copolymers as a function of time. All membranes are kept in 100 mM KCl.

4.3 Other Membranes: Equilibrium Hydration

Since swelling of polyelectrolyte membranes is significantly influenced by the pH of the bath solution, the hydration of other membranes being studied was measured under identical experimental conditions (pH and ionic strength) as the electroosmotic transport experiments. The results are shown in Table 4-2.

Membrane	thickness μm	Hydration @pH 7 g/g
S.1 75/25 DMAEMA/MMA	520	32.1
S.05/1 PMAA [1]	~100	27.9
5% carrageenan	520	13.7
4% 80/20 agarose/carr	500	15.6
1% calcium alginate	260	11.3
2% Ca alginate (B)	720	16.5
2% Ca alginate (C)	1640	25.1
2% agarose	620	18.8

Table 4.2: Equilibrium hydration (g solvent per g dry membrane) and thickness of membranes at pH 7. All are kept in 100 mM KCl with 1 mM potassium phosphate (except DMAEMA/MMA).

With the assumption that alginic acid contains the most charge followed by carrageenan and the synthetic polymers, the hydration shows no direct correlation with relative charge density. Swelling is governed by the interplay between electrostatic repulsion forces between membrane charge groups and the restoring force of the crosslinks. The wide deviation in hydration and the absence of correlation between hydration and relative charge density may also have been influenced by the nonuniformities in temperature between the different glass jars and slight differences in pH. It is noteable that all membranes, especially the calcium alginate were more swollen at the end of the transport experiments than before these hydration measurements were taken many days later on the same membrane. Adler (1988) had reported that hydration values were more consistent after the gels had been charged and neutralized once.

[1]The hydration value for PMAA is estimated from Grimshaw(1989) with units converted to g/g based on the polymer density given in the thesis.

Chapter 5

Experimental Results: Electroosmotic Solvent Flux

Using the apparatus of Figure 3-3, the solvent transmembrane flux was measured in response to an external pressure gradient or applied electric field. The experimental data was recorded as the total volume of solvent in the beaker versus time. Since the upstream and downstream chambers of the transport cell were completely filled with solvent, flow rates were measured as the change in weight of solvent in a covered beaker. For a given transmembrane current density a steady state transmembrane solvent velocity **U** (m/s) was attained and calculated as the change in volume V in the beaker over time, normalized by the membrane area A (3.14 cm^2).

$$U = \frac{1}{A}\frac{\partial V}{\partial t} \tag{5.1}$$

The electroosmotic coupling coefficient may be calculated using Darcy's Law (Eqn 3.1) and assuming that no internal pressure gradients exists ($\frac{\partial P}{\partial x} = 0$). With these assumptions, k_i is the slope of the flow rate for a given current density.

$$k_i = (\frac{\partial U}{\partial J})_{\nabla p=0} \tag{5.2}$$

When no internal or external pressure gradients exist across the membrane $k_i = \frac{U}{J}$

5.1 Electrically modulated transport in homogeneous membranes

For each experiment the difference in solvent height, $\triangle$h, was kept constant and recorded upstream to downstream so that the pressure drop across the membrane can be calculated as

$$\frac{\partial P}{\partial x} = \frac{\rho g \triangle h}{\delta} \tag{5.3}$$

The positive field is also defined upstream to downstream.

Solvent Flux across 75/25 DMAEMA/MMA. Transport experiments were conducted on a DMAEMA/MMA membrane to estimate the amount of electroosmotically induced flux. Using the apparatus of Figure 3-3 a slight, unmeasured pressure gradient was imposed across the membrane to keep it bowed in one direction. With both baths at pH 6.8 to 7, unbuffered, solvent always flowed downstream to upstream (Figure 5-1) upon application of a transmembrane field. Application of a positive current enhanced flow in the direction of the pressure gradient as negatively-charged counterions move opposite the applied field. At zero field the solvent flowed at a rate of 2.3 x 10^{-7} m/s to 3.1 x 10^{-7} m/s and increased 8 to 11-fold to 2.6 x 10^{-6} m/s with an applied field of 200 A/m^2.

Solvent Flux across carrageenan and agarose membranes. Using carrageenan and agarose/carrageenan membranes, repeatable flow rates were observed upon application of an electric field. In both experiments a constant difference in pressure was maintained between the upstream and downstream cells. As seen in figure 5-2, the flux changes were significantly higher in the 5% carrageenan than in the 4% 80/20 agarose/carrageenan. This experiment demonstrated a high correlation between fixed charge density and electrically induced solvent flux. If we assume that agarose contains no fixed charges and that all membrane charge is derived from carrageenan, the 5% carrageenan contains five times the charge density of the

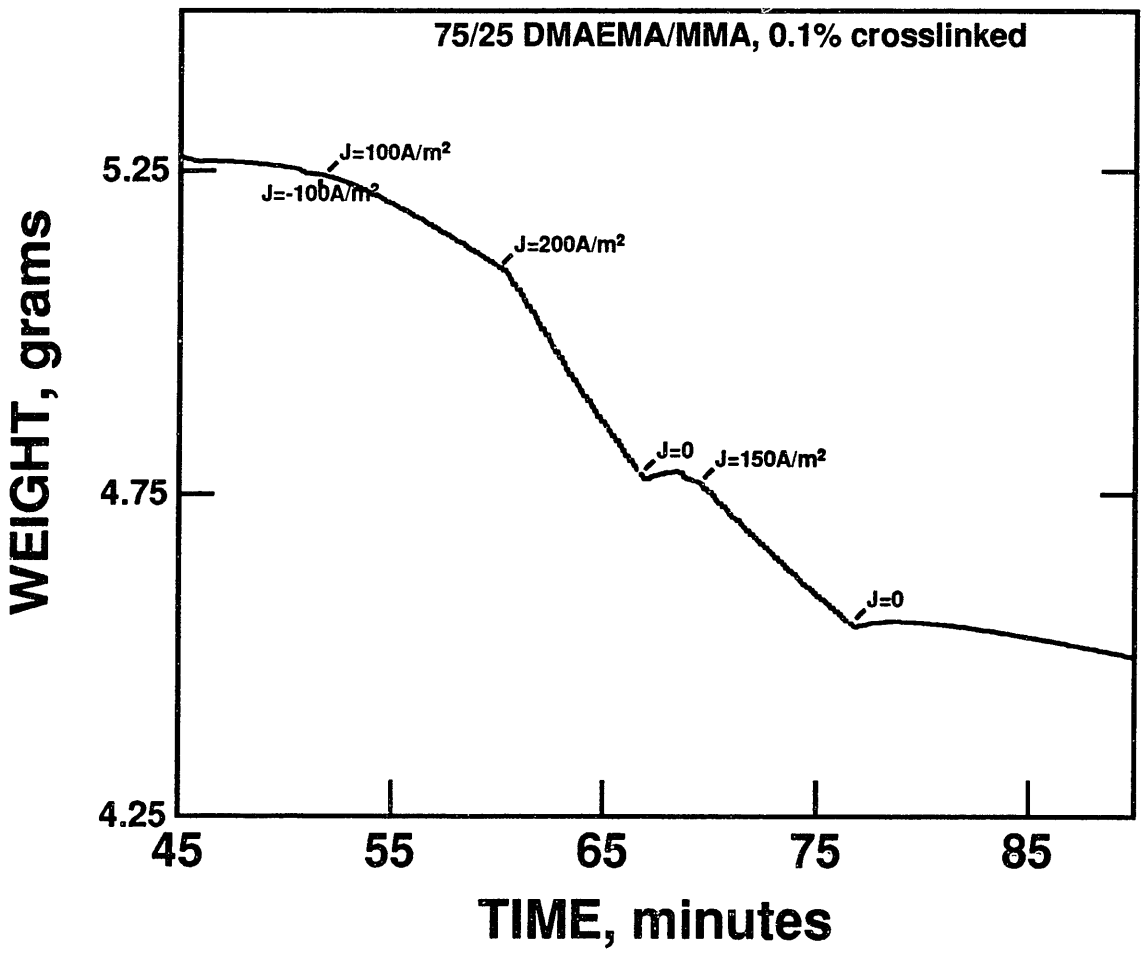

Figure 5-1: Electroosmotically induced flux across 75/25 DMAEMA/MMA with 0.1% crosslinker in 100 mM KCl. The upstream side of the bath was left open to the atmosphere so a fluid gradient of 2 to 3 cm was imposed on the membrane.

4% 80/20 agarose/carrageenan sample. Since manufacturer analysis of both products indicate that agarose contains <0.35% sulfate and carrageenan contains 7.34% sulfate (specific to this lot), the assumptions are even more reasonable.

The flow rates appeared to remain consistent even in the absence of an electric field because the constant pressure head minimized deviation for zero-field flow where the primary driving force was the external pressure gradient. For 5% κ-carrageenan the zero field flow rate of -1.6 x 10^{-7} m/s increased 30-fold to +4.8 x 10^{-6} m/s with an applied current density of -300 A/m^2. With the field decreased to -100 A/m^2, the flow rate decreased by about one-third to -1.6 x 10^{-6} m/s. The zero field flux then settled to a value 2 times higher than its initial value. The 4% 80/20 agarose/carrageenan membrane, with a 1 cm fluid gradient had a zero field flux of -1.4 x 10^{-7} m/s, increasing by a factor of 4.5 to -6.1 x 10^{-7} m/s with an applied field of -300 A/m^2. Applying 300 A/m^2 across the membrane caused a flow rate of 1.1 x 10^{-6} m/s, a flow ten times higher than the flow when the field is subsequently turned off. Although a fluid gradient of 7 cm was attempted, leakage from the electrodes prevented accurate measure of solvent flux.

5.2 Electrically modulated transport across Ca-alginate membranes

Because calcium alginate membranes are ideal for cell encapsulation and cell harvest but since its formulation does not necessarily create a uniform membrane, transport experiments were conducted to measure steady state flow and repeatability.

1% Ca alginate. Figure 5-3 shows the electroosmotic flux of 100 mM KCl with buffer at pH 7 through a 1% Ca-alginate membrane. The results, though repeatable, were unexpected. For a -300A/m^2 current density, a solvent flux of +7.8 x 10^{-7} m/s was measured while a flow of -4.8 x 10^{-7} m/s was measured for a field of the same magnitude in the opposite direction. These are, respectivly, 3 times and 1.5 times the magnitude of the zero field flow of 3.0 x 10^{-7} m/s. For a negatively-charged membrane electroosmotic flux should be augmented in

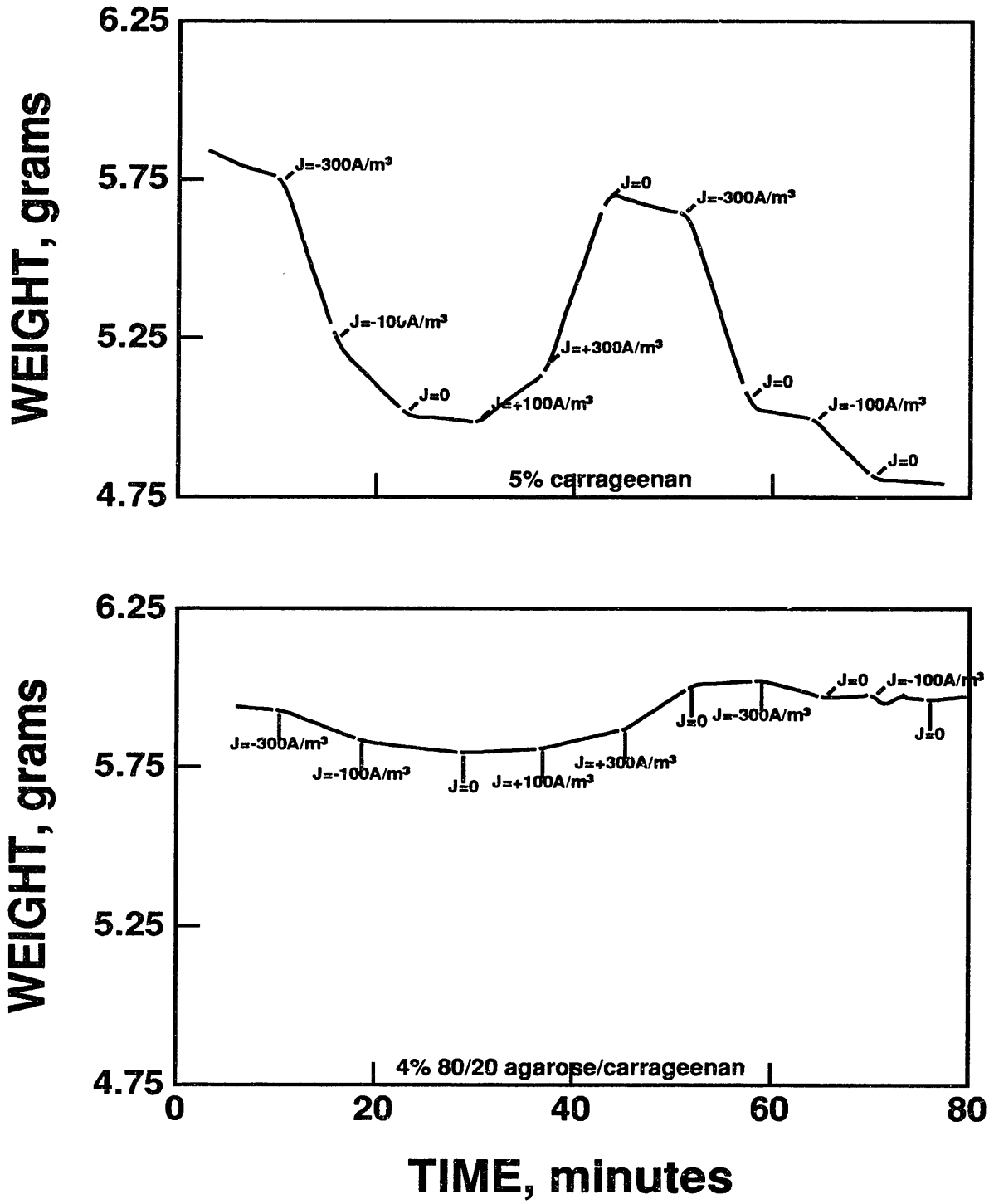

Figure 5-2: Cumulative volume of solvent transferred versus time for electroosmotic flow across a pure carrageenan and agarose/carrageenan hydrogel membrane. Membranes are in 100 mM KCl with 1 mM potassium phosphate at pH 7. Applied current densities are as labeled applied in the order -300 A/m^2, -100 A/m^2, 0 A/m^2, 100 A/m^2, and 300 A/m^2. Current densities were subsequently repeated. All flow rates are tabulated in Table 5-1.

the direction of the applied field, suggesting that this particular membrane may have a net positive charge. Solvent flux for two different pressure gradients were also measured: for $\triangle h$ = -2.3 cm, a flow of 1.3 x 10^{-5} m/s was observed and for $\triangle h$ = -29.3 cm, fluid flow was 1.0 x 10^{-4} m/s. However, the membrane broke under the pressure of the second pressure gradient and was disintegrating in the first so the result is of uncertain value. In fact several attempted experiments were aborted when the alginate membranes broke under the fluid pressure.

2% Ca alginate. Although the 2% calcium alginate formulation is tougher than the 1%, similar problems with membrane breakage occurred. It appeared that either the electric field or the concomitant flux would disrupt the electrostatic bonds between polymer groups, leading to granulation of the membrane. The round, disparate clusters easily dissociated from one another.

Consequently, many experiments were conducted with different 2% calcium alginate membranes. I have chosen to include three of them because they illustrate properties of the membrane. Note that the composition or mesh size of each membrane may not be the same, depending on the rate of diffusion of calcium into the alginate, the solution pH, and stoichiometry during each membrane's synthesis. In the first membrane (A), 1040 μm thick, electrically-induced flux on the order of 10^{-8} m/s was obs erved , suggesting an uncharged membrane. The experiment is shown in Figure 5-4A.

With the hypothesis that the calcium cation could potentially shield and neutralize all alginate carboxyl groups, a second membrane (B) was swollen in deionized water to twice its original thickness, re-equilibrated in 100 mM KCl at pH 7, and then its electroosmotic flux was measured. This membrane was mechanically backed by a piece of filter paper (Millipore Co, cellulose acetate, 8 μm pore size) on the upstream side to prevent breakage in measuring pressure-induced flux. Initial results were encouraging, with an observed flow of -3.8 x $10^{6} m/s$ with an applied current density of -300 A/m^2, 13 times higher than the zero field flow of 2.9 x $10^{-7} m/s$. After a few minutes (T=15 minutes) the back pressure reversed the flow direction and the membrane crumbled into the upstream side (Figure 5-4B).

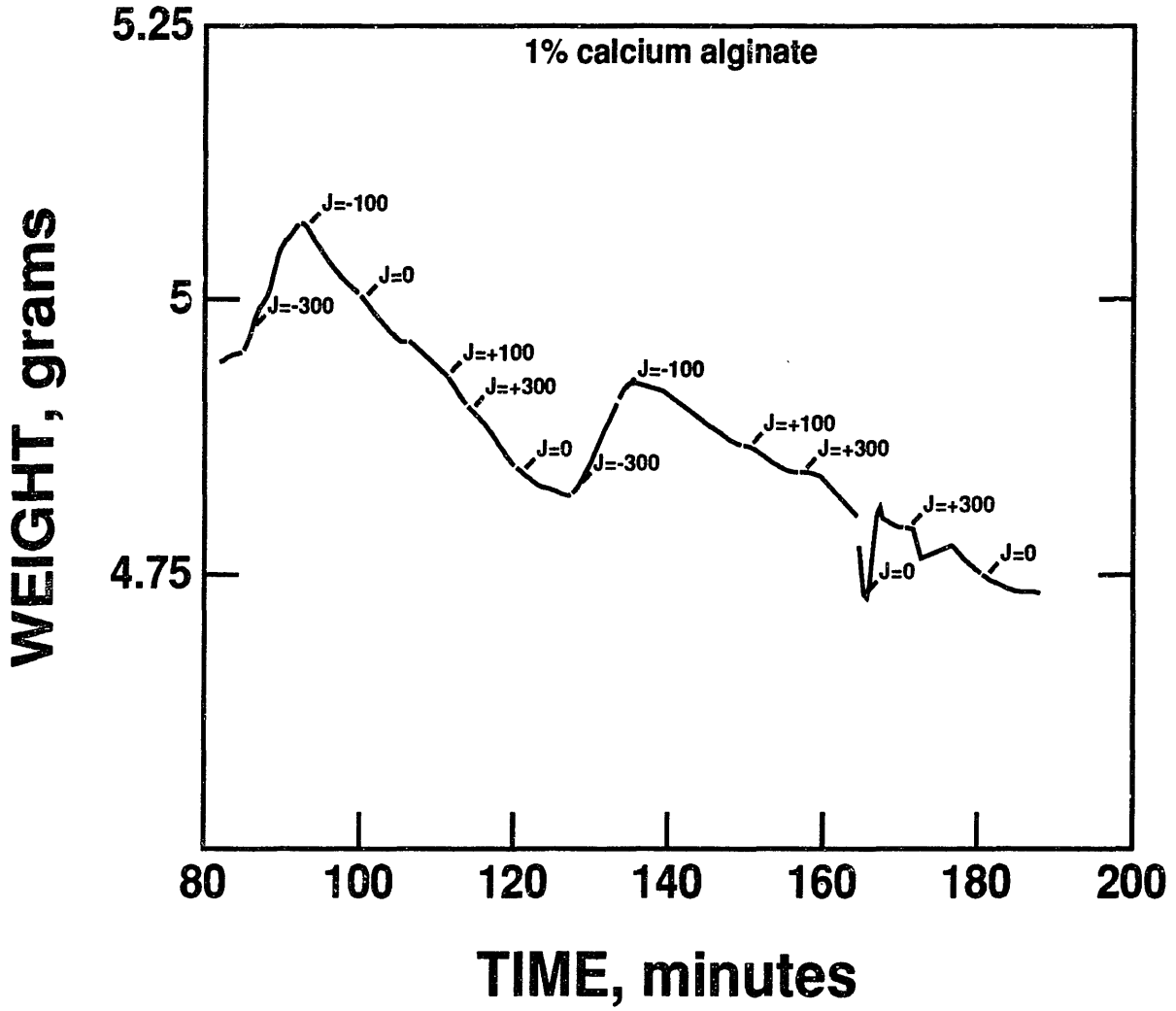

Figure 5-3: Electroosmotically induced flux across 1% alginate· 1% $CaCl_2$ in 100 mM KCl and 1 mM buffer at pH 7. The units of current density are A/m^2.

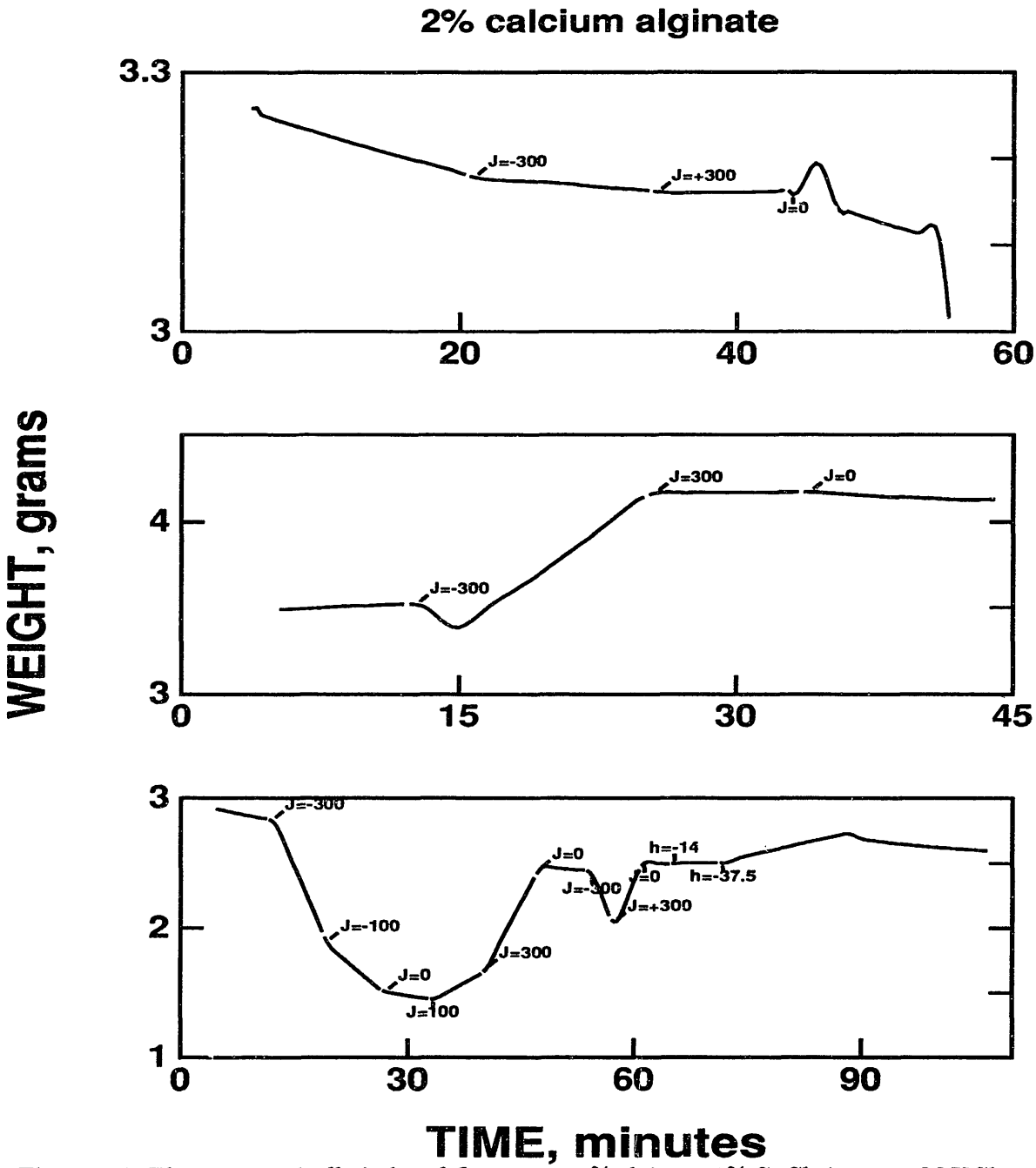

Figure 5-4: Electroosmotically induced flux across 2% alginate·1% $CaCl_2$ in 100 mM KCl and 1 mM buffer at pH 7. (A) Transport measured after synthesis and equilibration, $\triangle h = 0.6$ cm (B) Pre-swollen membrane with downstream side mechanically blocked, $\triangle h = -1.0$ cm (C) Pre-swollen membrane mechanically blocked on upstream and downstream sides, $\triangle h = -1.0$ cm. The units of current density are A/m^2.

In a third experiment, the pre-swollen, pre-equilibrated membrane (C) was mechanically backed with filter paper on both the upstream and downstream sides of the membrane before beginning the experiment. Large, fairly repeatable electroosmotic flow rates were observed (Figure 5-4C). A zero-field flow rate of -6.0 x $10^{-7} m/s$ was increased 12-fold to -7.2 x $10^{-6} m/s$ with a current density of -300A/m^2. Flow appeared to be proportional to the applied field strength with the -300 A/m^2 flow approximately 3 times higher than the -100 A/m^2 flow. The 100 A/m^2 flow of 1.7 x $10^{-6} m/s$ was 7 times the zero field flow rate, increasing three-fold to 5.9 x $10^{-6} m/s$ for an applied current of 300 A/m^2 . When the field is reapplied at -300 A/m^2, the flow is similar to that measured previously but when the direction is reversed, the measured flow increased by 25%. This increase in flow may reflect increases in pore size due to granulation.

To measure hydraulic permeability, a flow of 7.0 x $10^{-7} m/s$ was measured with a fluid gradient of -37.5 cm. With a fluid gradient of -14 cm flow rate varied from 1.2 x 10^{-8} to 4.9 x $10^{-8} m/s$. The final zero-current, -1.0 cm fluid gradient flow was 2.8 x $10^{-7} m/s$. Upon dissembling the transport apparatus the membrane was indeed granular and had expanded to approximately 2.5 times its original thickness. Though the high electrically- induced flux attests to the high charge density of the membrane, the final form of the membrane suggests that it may be too fragile for the forces imposed on it.

5.3 Transport across a neutral membrane

2% agarose. Electroosmotically induced flow through a neutral 2% agarose membrane was measured as a negative control since a membrane carrying essentially no intrinsic charge is not expected to influence solvent flux upon application of a transmembrane electric field. The flow, with or without an applied field, ranged between 1.9 x 10^{-7} to 2.7 x $10^{-7} m/s$ with no apparent correlation between flow and applied current density. With a fluid gradient of -18.5 cm a flow of 1.4 x $10^{-5} m/s$ was measured.

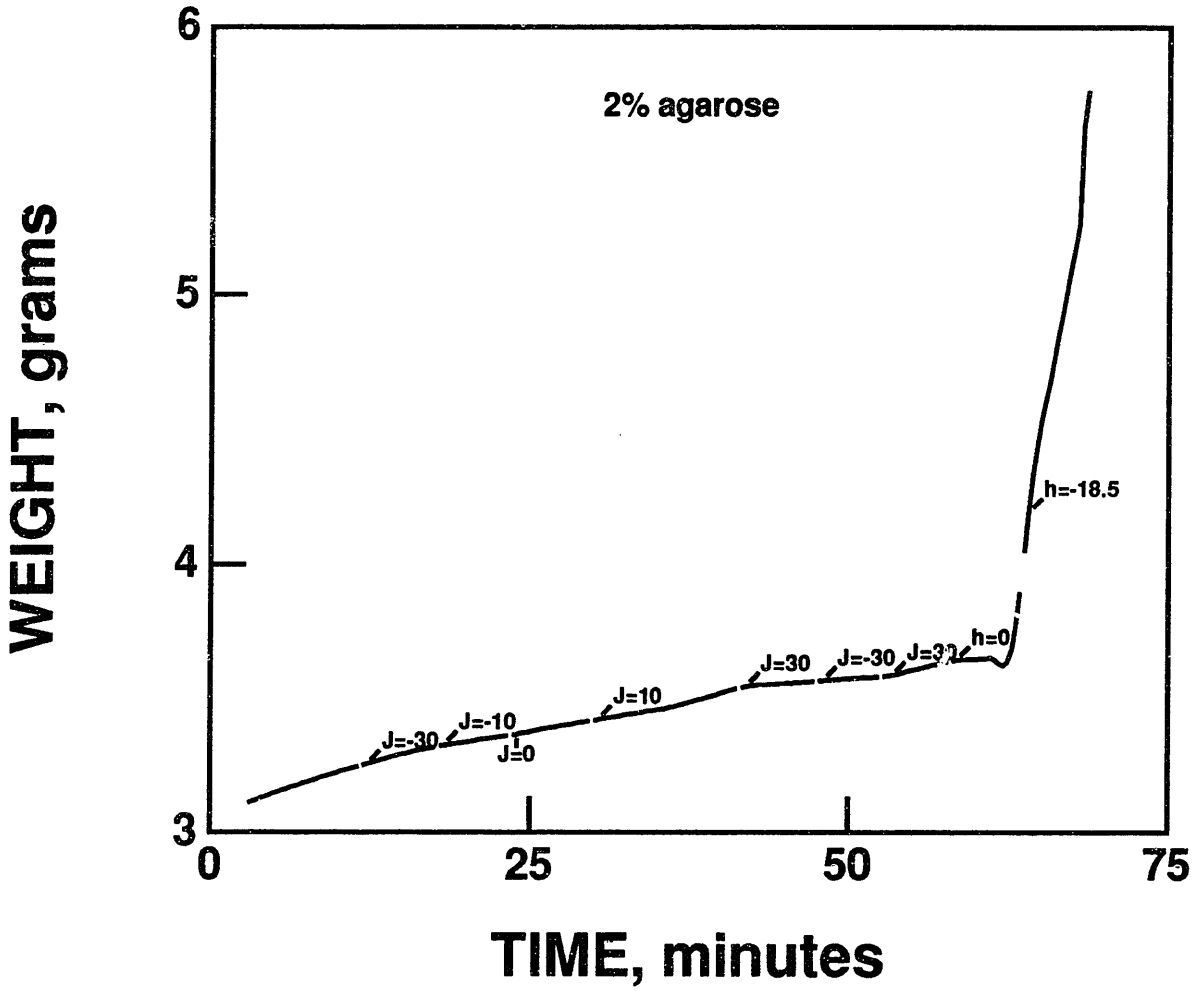

Figure 5-5: Electroosmotically induced flux across 2% agarose membranes in 100 mM KCl and 1 mM buffer at pH 7. Mechanical barriers (filter paper) were placed on upstream and downstream sides of the membrane. Initially, no pressure gradient was applied across the membrane.

5.4 Summary of Transport Experiment Flow Rates

Transmembrane solvent velocities U, calculated from the data of Figure 5-1 to Figure 5-4 using equation 5.1, are recorded in Table 5.1. The sequence of applying field strengths shown in the figures is the same as the sequence of tabulated flow rates except when flow fluctuated too much to measure an accurate slope.

The zero-field flow rates are different from membrane to membrane, dependent on the external pressure gradient across the membrane and the membrane's hydraulic permeability. An upstream to downstream pressure gradient was chosen so that some solvent flow was observed and the membrane kept taunt. Since a constant pressure drop was not maintained across the 75/25 DMAEMA/MMA membrane a linear relation between flow rate and applied current density may not be observed. In cases where the solvent flux was relatively fast, such as the 2% alginate (C), it was difficult to constantly watch the fluid height; in that case, comparing the electroosmotically-induced flux to the associated zero-field flux is most accurate.

MEMBRANE	Δh (cm)	FLOW RATE (μm/sec)					
		0 A/m²	-300 A/m²	-100 A/m²	0 A/m²	+100 A/m²	+300 A/m²
S.1 75/25 DMAEMA/MMA	-(2 to 3)			-0.61	-0.31 -0.23	0.92	2.6
5% carrageenan	-0.5	-0.16	-4.8 -4.9	-1.6 -1.6	-0.37 -0.37	1.2	4.8
4% 80/20 agarose/ carrageenan	-1.0	-0.14	-0.61	-0.19	0.090 0.11	0.39 0.41	1.1 1.0
1% Ca-alginate	0	 -0.15	0.78 0.80	-0.47 -0.22	-0.38 -0.22	-0.58 -0.53	-0.48 -0.43
2% Ca-alginate(A)	0.6	-0.25	-0.060		-0.26		0.011
2% Ca-alginate (B)	-1.0	0.25	-3.8 4.1		-0.29		0.010 0.018
2% Ca-alginate (C)	-1.0	-0.60 -0.26	-7.2 -7.1	-2.6	-0.51 -0.28	1.7	5.9 7.4
2% agarose	0	0.82 0.19	0.64 0.17	0.37	0.45	0.42 0.63	0.72

Table 5.1: Electrical control of solute flux across uniform membranes in 100 mM KCl buffered with 1 mM potassium phosphate at pH 7. Flow rate is calculated using Equation 5-1 and measured during application of E-fields of different strengths applied in the order shown in the table and illustrated in Figures 5-1 to 5-5.

Chapter 6

Interpretation of Results

6.1 Electroosmotic Coupling Coefficient

Using equation 2.3, the electroosmotic coupling coefficient, or the relation between flow rate U and current density J, was calculated. These calculations were based upon the average solvent flow for an applied current density.

The field contribution to flow for carrageenan and agarose/carrageenan, shown in figure 6-1, indicates a linear relation between current density and flow. The electroosmotic coupling coefficients for 5% carrageenan is 1.6 x10^{-8} $m^3/sec{\cdot}A$, 5.7 times greater than the calculated coefficient of 2.8 x 10^{-9} $m^3/sec{\cdot}A$ for 4% 80/20 agarose/carrageenan. The difference in electroosmotic coupling parallels the difference in associated charge between the two polymers since 5% carrageenan has 6 times the charge density of 4% 80/20 agarose/carrageenan. The 4% 80/20 agarose/carrageenan has roughly half the electroosmotically induced flux measured by S.1 75/25 DMAEMA/MMA, putting it in the same order of magnitude as S.05/1 PMAA as well.

The electroosmotic coupling of flow to current density for alginate is shown in Figure 6-2. The result is linear for one experiment of 2% calcium alginate while the 1% Ca alginate behaved irregularly. It was expected that the electroosmotic coupling of 2% calcium alginate should be approximately twice that of a hydrogel of 1% calcium alginate. However, the instability of the membrane makes it uncertain that even the same membrane placed in a bath would give consistent results.

Comparisons of all membranes studied are shown in Figure 6-3. The preswollen 2% Ca alginate showed the greatest electrical augmentation of flux followed by 5% carrageenan. Results from electroosmosis through 1% Ca alginate were unclear. S.1 75/25 DMAEMA/MMA revealed a nonlinear relation to current density consistent where depending on the current density a different local slope was observed; the negative relation between increasing current density and volume flow is consistent with the positive charge of the membrane. 4% 80/20 agarose/carrageenan showed a slight effect, and 2% agarose had a flat profile.

The calcium alginate membranes gave unusual results, bringing up the question of intrinsic membrane charge density. With the crosslinking of calcium alginate created by divalent calcium cation bonding between two carboxyl groups, the possibility arises that calcium can partially or fully neutralize the negative charge in alginic acid in the process of forming a gel. Since binding of calcium is reversible, it is also conceivable that potassium shielding may release some calcium bonds with the end result being the observed granulation of a previously smooth membrane. Although carrageenan hydrogels may be formed by shielding its sulfate groups with potassium to enable hydrogen bonding, use of potassium as the principal cation in the transport experiments does not seem to affect electroosmotic transport by carrageenan; the flow rates remain consistent and the membrane is unchanged by the transport experiment.

Summary of Electroosmotic Coupling Coefficients. The electroosmotic coupling coefficient is calculated as the slope of the relation between U and J from Figures 6-1 and 6-2. The results are listed in Table 6.1.

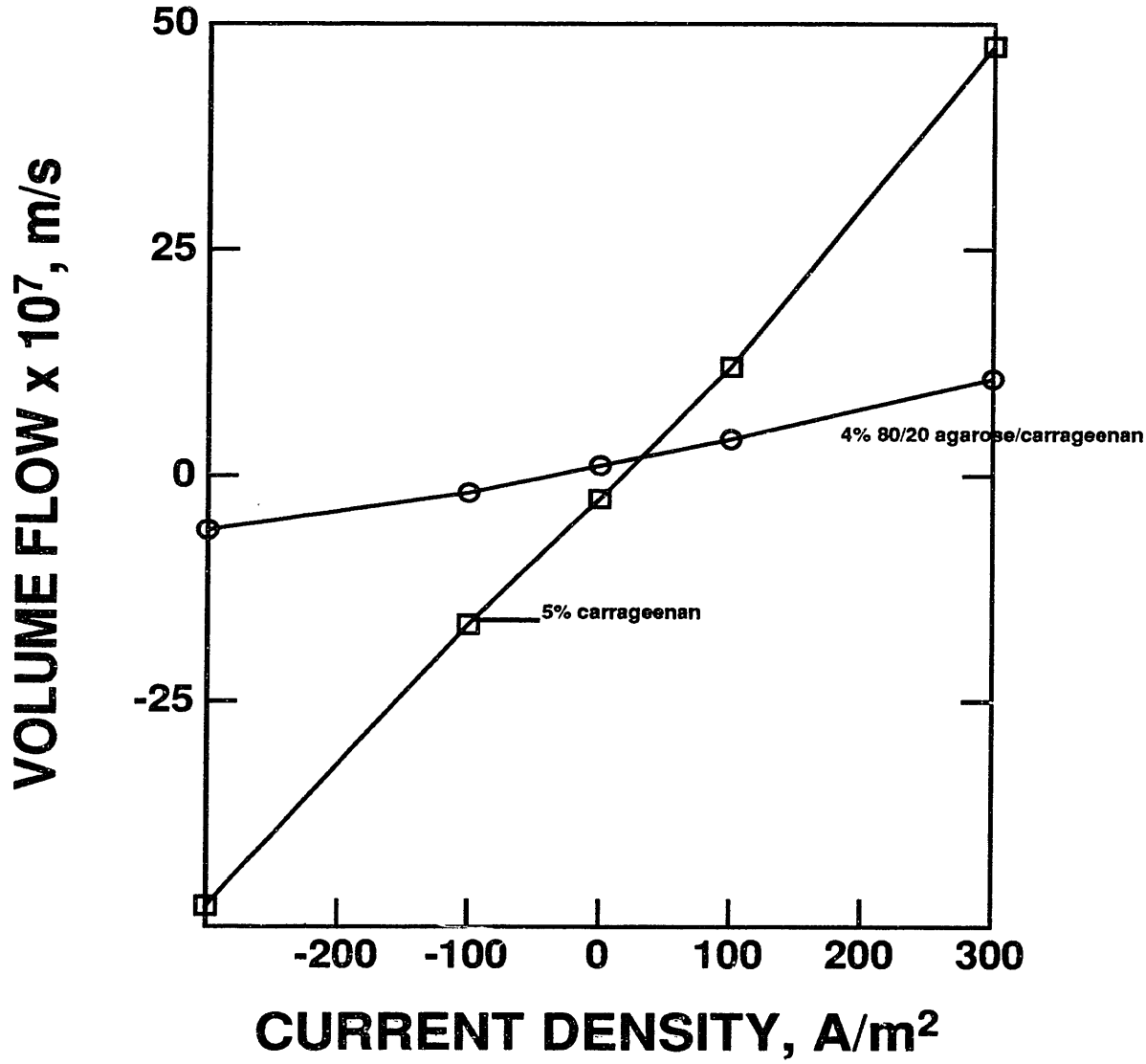

Figure 6-1: Flow rate versus current density for carrageenan based membranes. 5% carrageenan (□) and 4% 80/20 agarose/carrageenan (○) membranes 500μm thick were used 100 mM KCl and 1 mM phosphate. Data is taken from Figure 5-2.

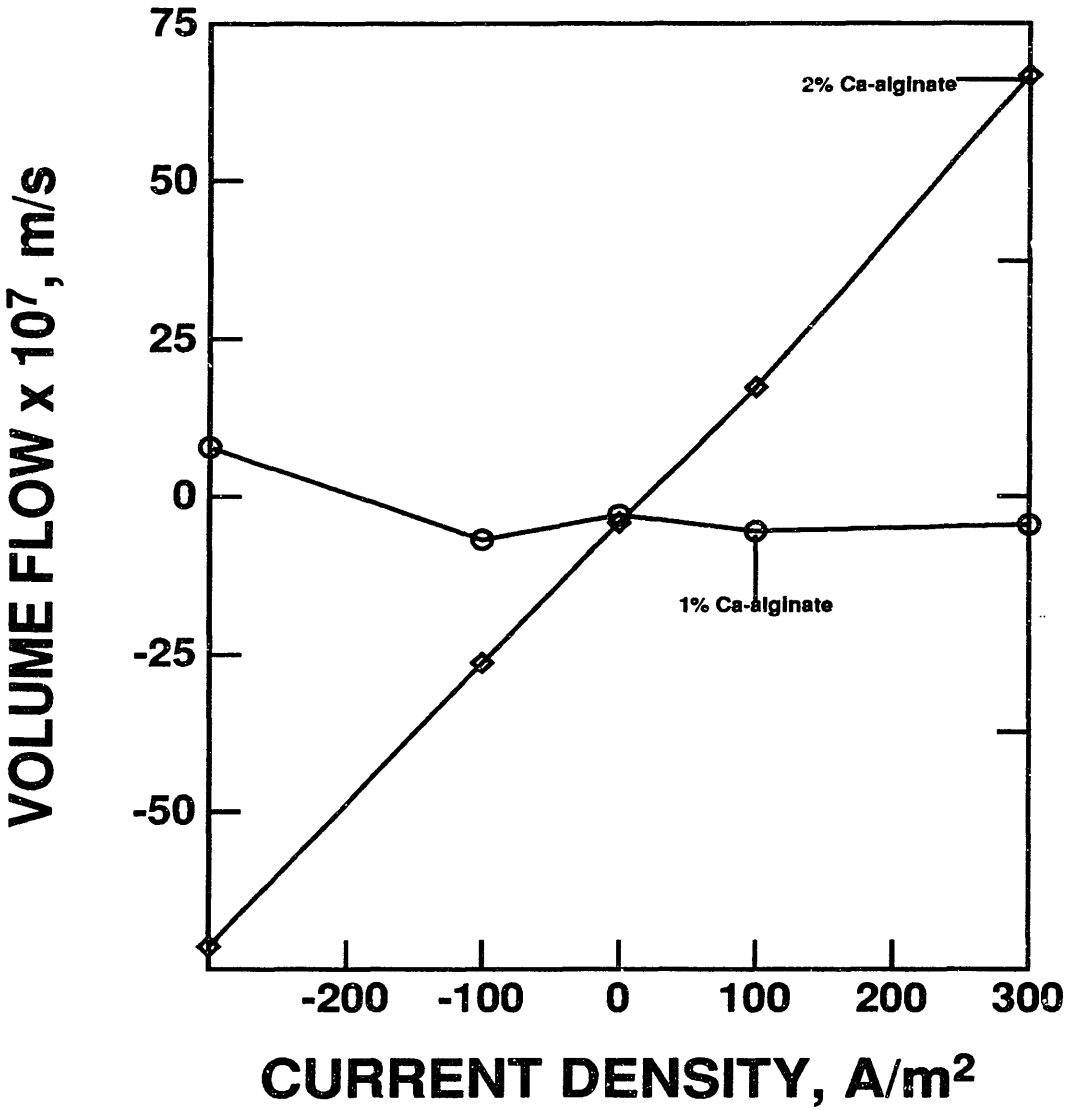

Figure 6-2: Flow rate versus current density for alginate based membranes. 1% Ca alginate (○) and 2% calcium alginate (◇) membranes 260 to 1640 μm thick were used 100 mM KCl and 1 mM phosphate. Data is taken from figure 5-3 and figure 5-4(C).

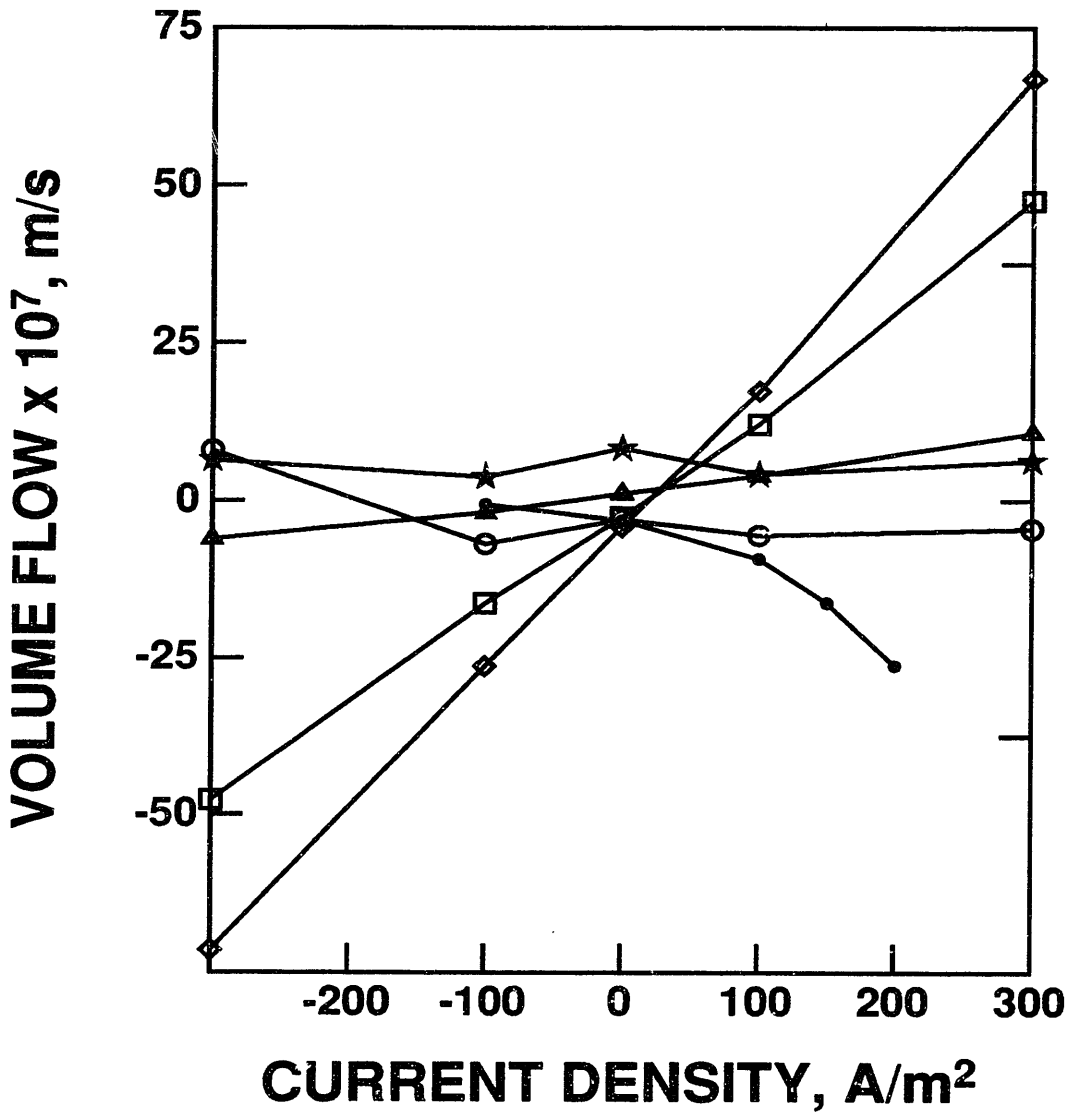

Figure 6-3: Flows associated with transmembrane current densities shown for all membranes studied. Flow rates are taken from figures 5-1 to 5-5. From outside inwards is 2% Ca alginate ($\diamond$), 5% carrageenan ($\square$), 4% 80/20 agarose/carrageenan ($\triangle$), S.1 75/25 DMAEMA/MMA ($\bullet$), 1% Ca alginate ($\bigcirc$), and 2% agarose ($\star$).

Membrane	pH	k_i $m^3/sec \cdot A$
S.1 75/25 DMAEMA/MMA	6.8 to 7.0	5.87 x 10^{-9}
S.05/1 PMAA	7.0	3.2 x 10^{-9}
5% carrageenan	7.0	1.57 x 10^{-8}
4% 80/20 ag/carr	7.0	2.80 x 10^{-9}
1% Ca alginate	7.0	1.97 x 10^{-9}
2% Ca alginate	7.0	2.19 x 10^{-8}
2% agarose	7.0	5.70 x 10^{-13}

Table 6.1: Summary of Calculated Electroosmotic Coupling Coefficients

Membrane	$\triangle h$ (cm)	δ (μm)	$\frac{\partial P}{\partial x}$ $(10^{-8}N/m^3)$	U for $\frac{\partial P}{\partial x}$ $(\mu m/s)$	k' $(10^{16}m^4/N \cdot s)$
S.1 75/25 DMAEMA/MMA	-2	520	3.92	-0.270	6.89
	to -3		5.88		1.44
5% carrageenan	-0.5	520	0.942	-0.369	39.2
4% 80/20 agarose/carr	-1.0	500	1.96	0.0979	4.99
1% Ca alginate	-2.3	260	8.67	-13.19	152
2% Ca alginate	-37.5	1640	22.4	-0.700	3.13
2% agarose	-18.5	620	29.2	-14.0	47.9

Table 6.2: Summary of Calculated Hydraulic Permeability

6.2 Hydraulic Permeability Coefficient

The hydraulic permeability is a reflection of the pore size of the various membranes. It is calculated for a zero-field flow rate for a known pressure gradient using equation 2.1. The pressure gradient $\frac{\partial P}{\partial x}$ was calculated using equation 5.3 with the assumption that solvent density $\rho = 10^3 kg/m^3$, gravitational constant g = 9.8 m/s^2, and δ was the measured, equilibrated membrane thickness from Table 4-2. The results are tabulated in Table 6.2.

Membrane	$\bar{\rho}_m^{max}$ (mol/l)	k_i ($m^3/sec \cdot A$)	k' ($m^4/N \cdot s$)	ϕ @ pH 7 (g/g)
S.1 75/25 DMAEMA/MMA	3.66	5.87 x 10^{-9}	5.47 x 10^{-16}	0.970
S.05/1 PMAA	-0.415	3.2 x 10^{-9}	2.7 x 10^{-16}	0.965
5% carrageenan	-0.130	1.57 x 10^{-8}	3.92 x 10^{-15}	0.931
4% 80/20 ag/carr	-0.0258	2.80 x 10^{-9}	4.99 x 10^{-16}	0.940
1% Ca alginate [2]	-0.0571	1.97 x 10^{-9}		0.919
2% Ca alginate	-0.114	2.19 x 10^{-8}	3.13 x 10^{-16}	0.962
2% agarose	0	5.70 x 10^{-13}	4.79 x 10^{-15}	0.949

Table 6.3: Summary of Calculated Membrane Charge Density

6.3 Charge Density

The charge density of natural polymers can be estimated from the amount of dry powder, the water used to synthesize each membrane, and the molecular weight of each "monomer." By computing that each monomer unit contributes one net negative, positive, or neutral charge, a calculation can be made for an upper limit in membrane charge density where all ionizable groups are assumed to be ionized. The estimate of charge density is fairly reasonable since at pH 7 sulfate groups should all be ionized and carboxyl groups should mostly be ionized. For natural membranes, maximum charge density was calculated by dividing polymer density by molecular weight and hydration. Since the polymer density of DMAEMA/MMA was not known, the calculated membrane charge deviates by the square of its dry polymer density. The calculation, the upper limit on charge density, is denoted by $\bar{\rho}_m^{max}$. The calculated values are tabulated in Table 6.3.

Charge density can also be solved using equation (2.4) and values measured for k_i and k'. The membrane water content ϕ can be calculated from the hydration measurements and the intramembrane ionic concentration $\bar{c}_i$ can be calculated using Donnan partitioning. Values for k_i, k_f, and ϕ are listed in Table 6.3.

According to manufacturer analysis of the chemicals, κ-carrageenan contains 28.5% C, 4.06% H, 0.7% Na, 3.6% K, 2.9% Ca, and 7.34% S. The sodium alginic acid contains 31.2%C,

[2]The hydraulic permeability for 1% calcium alginate was calculated to be 1.52 x $10^{-14} m^3/sec \cdot A$ but is believed to be high because of the granulation of the membrane.

Solute	Diffusivity [3] $(10^5 cm^2/s)$ @ 25^oC
oxygen	2.41
glucose	0.69
lactate	1.10
urea	1.38

Table 6.4: Diffusivities of Cell Nutrients and Waste Products.

4.12%H, and 14.9% Na. Since sodium alginic acid is formed by addition of sodium to shield carboxyl groups and break bonds between side chains, the net negative charge is approximately 14.9%. The charge of carrageenan comes primarily from sulfate groups, giving a net negative charge of approximately 7.34% or about half the alginic acid charge for a given weight dry powder.

6.4 Peclet Number

Using the diffusivities for common cell nutrients and waste products listed in Table 6.4, the combined electrophoretic and electroosmotic flux augmentation in the peclet number can be calculated for transport across each type of membrane. The electroosmotically augmented flux component of Peclet is calculated using membrane thickness δ, porosity ϕ, solute diffusivity, and field-induced flow and tabulated in Table 6.5. According to the data, significant solute flux augmentation is possible through 2% calcium alginate, 5% carrageenan, and S.1 75/25 DMAEMA/MMA. The Peclet number for S.05/1 PMAA is in the order of 1, putting it in the same order of magnitude as S.1 75/25 DMAEMA/MMA (Grimshaw, 1989). Note that the 2% calcium alginate yields Peclet number 4 times that of 5% carrageenan, a factor that may not be readily observed from the electroosmotic flow rates.

[3] Values taken from Chang (1990).

MEMBRANE	Peclet for J=300A/m^2 flow			
	oxygen	glucose	lactate	urea
S.1 75/25 DMAEMA/MMA	0.584	2.04	1.28	1.02
5% carrageenan	1.10	3.85	2.42	1.92
4% 80/20 agarose/carr	0.234	0.817	0.513	0.409
1% Ca alginate	0.0533	0.186	0.116	0.0930
2% Ca alginate	4.72	16.5	10.4	8.25
2% agarose	0.195	0.0506	0.428	0.341

Table 6.5: Peclet numbers for maximum measured flow rates

Chapter 7

Conclusions

7.1 Summary

Solute flux through synthetic and natural hydrogels were studied. Originally chemical control of swelling, or charge density, was investigated for DMAEMA/MMA copolymers where the swelling transition occurred around pH 7. The synthetic copolymer most compatible with cell immobilization and culture media, S.1 75/25 DMAEMA/MMA, showed flux rates magnified by 9.8 with a positive field and by 2 with a negative field. The other hydrogels included for characterization have carboxyl and sulfate charge groups, groups that are almost completely ionized at physiological pH. Therefore, bath ionic content, a factor that would not significantly affect charge, was kept constant and membrane composition was used as the variable for establishing charge density.

Measurements were made using two primary systems: carrageenan and calcium alginate membranes. Agarose, a neutral hydrogel, was used to vary the carrageenan charge and also as a negative control. Exact polymer concentrations were chosen in a range that had been used to immobilize cells. For carrageenan, solvent flux was augmented by electroosmosis by

factors in the range 8.4 to 13.9, for the current densities used. For the calcium alginate, the range was 3.7 to 17.8 times the zero field flux.

Measurement and analysis for PMAA, conducted by Grimshaw (1989) were included as a representative negatively-charged synthetic membrane. His calculations also serve as a valuable comparison.

Measured flux was analyzed in the context of a one-dimensional continuum model to calculate parameters related to solvent transport and to determine the implications on solute transport. From calculation of electroosmotic contribution to the Peclet number, only the 5% carrageenan, the 2% calcium alginate, and S.1 75/25 DMAEMA/MMA membranes gave significant augmentation of common cell nutrients and waste products.

7.2 Comparisons with previous work.

Although cell immobilization matrices are not new, use of electric fields to overcome diffusion-limitations and to augment transport through membranes filled with cells has not been previously studied. Therefore, comparisons for electrical augmentation can be made with other membrane systems such as PMAA which shows comparable permeabilities and electroosmotic coupling. In studying immobilized systems, factors to consider would be transport augmentation, facility of immobilization procedure, successful cell viability after immobilization, and other system-specific factors.

Transport augmentation in different membranes was the focus of this thesis. In the systems investigated, the electroosmotically enhanced flux was greater with calcium alginate membranes than through carrageenan membranes for the compositions studied. DMAEMA provided slightly less flux augmentation, but fared somewhat better than PMAA. For a porous enough membrane, the charge density appeared to be the largest determinant of electroosmotic flux. However, a systematic correlation of charge density, hydraulic permeability,

and electroosmotic coefficient remains to be done. In pressure-induced flux augmentation in carrageenan membranes, pure carrageenan was more porous than one formed from both agarose and carrageenan. Similarly and as would be expected, the alginate membrane that contained more alginic acid was less porous (more compact in structure) than the one with a higher water content. The calcium alginate varied over a larger range of hydraulic permeabilities than the carrageenan system, but both overlapped. However, the high degree of electroosmotic flux observed in both membrane systems makes it unlikely that either system would be flow-limiting.

A factor not quantitatively assessed here is the facility of immobilizing cells in a gel framework. In synthesizing each hydrogel, the physiological conditions to be considered for gelling include temperature, pH, and the presence of toxic chemicals. The strength of each membrane can also be a factor. Immediately, DMAEMA was be eliminated on this basis since the initiator is potentially harmful to cells. The carrageenan can be formed at physiological conditions with the addition of potassium salts. Calcium alginate is formed, through a different mechanism, by the addition of calcium ions to alginic acid. Both can be prepared in the mild conditions of room temperature and physiological pH. The softness of the prepared alginate gel make it seem unlikely that cells can be held together in a matrix made of this material without considering additional mechanical constraints.

Since hydrogel materials were chosen on the basis of biocompatibility and previous success in immobilizing cells, all materials studied were considered to potentially provide high cell viability. Other factors are specific to the need of cells in an immobilization matrix. For instance, in extracting products that remain in the cell, such as DNA, the ability to dissolve the gel to return whole cells would favor alginic acid.

These observations are based on membranes as they are synthesized under the conditions previously described. It would be valuable to further stipulate formation condition, in terms of pH, temperature, ionic content, to achieve higher repeability for measurement and consistency of membrane mesh size. The results that have been calculated and the flow rates observed remain useful for choosing a continuous range of flow rates for selective partitioning of solutes

where an approximate membrane composition can be estimated.

Based on observations of electroosmotic flux augmentation, membrane synthesis procedure, final membrane tensile strength to the forces imposed, and repeatability of results, carrageenan/agarose membranes have the greatest potential for reliable use as a cell immobilization matrix. Membrane composition, field strength, and bath pH can be controlled to give the desired range of flux augmentation of nutrient and waste products.

Bibliography

Adler, K.P., 1988. Correlation of Permeability, Hydration, and Crosslink Density in Polyelectrolyte Hydrogel Membranes. M.I.T. (M.S. thesis)

Baudet, C., J. Barbotin, and Guespin-Michel, 1983. Growth and Sporulation of Entrapped *Bacillus subtilis* Cells. *Applied and Environmental Microbiology*, **45(1)**: 297-301.

Chang, Y.H., 1990. Augmentation of Mass Transfer Through Electrical Means for Entrapped Animal Cell Bioreactor. M.I.T. (Ph.D. thesis proposal)

Cussler, E.L., 1988. Gels as Size Selective Extraction Solvents. Purdue University seminar.

Domurado, M., F. Deramoudt, and D. Thomas, 1988. Immobilization of murine lymphocytes by gel entrapment, *Biotechnology Techniques*, **2**: 211-216.

Duff, R.G., 1985. Microencapsulation technology: a novel method for monoclonal antibody production, *Trends in Biotechnolgy* **3**(7): 167-174.

Firestone, B.A. and R.A. Siegel, 1988. Dynamic pH-dependent Swelling Proerties of a Hydrophobic Polyelectrolyte Gel, *Polymer Communications*, **29**: 204-208.

FMC Corporation, 1988. FMC Bioproducts Sourcebook.

Frank, E.H. *et al.*, submitted 1990, Physiochemical and Bioelectrial Determinants of Cartilage Material Properties.

Freeman, A. and Aharonowitz, 1981. Immobilization of Microbial Cells in Crosslinked, Prepolymerized, Linear Polyacrylamide Gels: Antibiotic Production by Immobilized *Streptomyces clavuligerus* Cells. *Biotechn and Bioeng*, **23**: 2747-2759.

Freijtas, R. and E.L. Cussler, 1987. Temperature Sensitive Gels as Extraction Solvents, *Chemical Engineering Science*, **42**(1): 97-103.

Gehrke, S.H., G.P. Andrews, and E.L. Cussler, 1986. Chemical Aspects of Gel Extraction,

Chemical Engineering Science, **41**(8): 2153-2160.

Gehrke, S.H. and E.L. Cussler, 1989. Mass Transfer in pH-Sensitive Hydrogels, *Chemical Engineering Science*, **44**(3): 559-566.

Gharapetial, H., and M. Maleki, N.A. Davies, and A.M. Sun, 1986. Polyacrylate Membranes for Encapslation of Viable Cells, 11-118.

Gilligan, K.J., S. Littlefield, and A.P. Jarvis, 1987. Production of rat monoclonal antibody from rat x mouse hybridoma cell lines using microencapslation technology. *In Vitro Cellular and Developmental Biology* **24**(1): 35-41.

Grimshaw, P.E., 1989. Electrical Control of Solute Transport Across Polyelectrolyte Membranes, M.I.T. (Ph.D. thesis).

Grimshaw, P.E. and A.J. Grodzinsky, et. al., 1988. Dynamic Membranes for Protein Transport: Chemical and Electrical Control. *Chemical Engineering Science*, **43**(0): 1-14.

Grodsinsky, A.J. and J.R. Melcher, 1976. Electromechanical Transduction with Charged Polyelectrolyte Membranes, *IEEE Transactions on Biomedical Engineering*, **BME-23**(6): 421-433.

Grodzinsky, A.J. and Shoenfeld, N.A., 1977. Tensile Forces Induced in Collagen by Means of Electromechanochemical Transductive Coupling. *Polymer*, **18**: 435-443.

Hooper, H.H. *et al.*, 1990 (submitted). Swelling Equilibria for Positively Ionized Polyacrylamide Hydrogels.

Iijima, S., M. Takashi, M. Taniguchi, and T. Kobayashi, 1988. Immobilization of hybridoma cells with alginate and urethane polymer and improved monoclonal antibody production. *Appl Microbiol Biotechnol* **28**: 572-576.

Ilavsky, M., 1981. Effect of Electrostatic interactions of Phase Transition in the Swollen Polymeric Network, *Polymer*, **22**: 1687-1691.

Kelco, Inc., 1989. Algin: Hydrophilic derivitives of alginic acid for scientific water control. 2nd ed.

Krouwel, P.G., and A. Harder and N.W.F. Kossen, 1982. Tensile Stress-Strain Measurements of Materials Used for Immobilization. *0Biotechnology Letters*, **4(2)**: 103-108.

Lim, F. and A.M. Sun, 1980. Microencapslated islets as bioartificial endocrine pancreas, *Science* **210**: 908-910.

Morikawa, Y. and I Karube, and S Suzuki, 1980. Continuous Production of Bacitracin by Immobilized Whole Cells of *Bacillus sp.*, *Biotechn and Bioeng*, **22**: 1015-1023.

Mosbach, K. and Per-olof L., 1970. Preparation and Application of Polymer-entrapped enzymes and microorganisms. *Biotechnology and Bioengineering*, **12**: 19-27.

Nussbaum, Jermey Howard, 1986. Electric Field Control of Mechanical and Electrochemical Properties of Polyelectrolyte Gel Membranes. M.I.T. (Ph.D. thesis)

Ohmine, I., and T. Tanaka, 1982. Salt Effects on the Phase Transition of Ionic Gels, *J. Chem Phys*, **77**(11): 5625-5729.

Reinhart and Peppas, 1984. Solute Diffusion in Swollen Membranes. Pt II. Influence of Crosslinking on Diffusive Properties. *J. Membrane Sci.*, **18**: 227-239.

Sefton, M.V. *et al.*, 1987. Hydrophilic Polyacrylates for the Microencapsulation of Fibroblasts or Pancreatic Islets, *J. Controlled Release*, **6**: 177-187.

Shatayeva, L.K. and G.V. Samsonov, 1979. Permeability of Heterogeneous Membranes Based on Methacrylic Acid. *Journal of Applied Polymer Science*, **23**: 2245-2251.

Shatkay, A and I Michaeli, 1966. *J Phys Chem*, **70**: 3777.

Siegel, Ronald A., 1988. pH-Sensitive Gels: Swelling Equilibria, Kinetics, and Applications for Drug Delivery. UCSF Pharmaceutical Chemistry memo.

Siegel, R.A. and B.A. Firestone, 1988. pH-Dependent Equilibrium Swelling Properties of Hydrophobic Polyelectrolyte Copolymer Gels. *Macromolecules*, **21**: 3254-3259.

Siess, M.H. and C. Divies, 1981. Behavior of *Saccharomyces cerevisiae* Cells Entrapped in a Polyacrylamide Gel and Performing Alcoholic Fermentation. *J. Appl Microbiol Biotechnol*, **12**: 10-15.

Slowinski, W. and S.E. Charm, 1973. Glutamic Acid Production with Gel-entrapped *Corynebacterium glutamicum*, *Biotechnology and Bioenginering*, **15**: 973-979.

Tanaka, T. and D.J. Fillmore, 1979. Kinetics of Swelling of Gels, *J. Chem. Phys.*, **70**(03).

Tanaka, H., M. Matsumura, and I.A. Veliky, 1984. *Biotechnol. Bioeng.* **26**: 53-58.

Tompkins, R.G., E.A. Carter, J.D. Carlson, and M.L. Yarmush, 1988. Enzymatic Function of Alginate Immobilized Rat Hepatocytes, *Biotechnology and Bioengineering* **31**: 11-18.

Weiss, A.M. and A.J. Grodzinsky and M.L. Yarmush, 1986. Chemically and Electrically Controlled Membrnaes: Size Specific Transport of Fluorescent Solutes through PMAA Membranes *AIChE Symposium Series*, **82**(250): 85-98.

Yamamoto, K. and T. Tosa and I. Chibata, 1980. Continuous Productrion of l-Alanine Using *Pseudomonas dacunhae* Immobilized with Carrageenan. *Biotechnology and Bioengineering*, **22**: 2045-2054.